Aftershocks at Short Times After Large Earthquakes in Japan: Implications for Earthquake Triggering

Bogdan Enescu

Faculty of Life and Environmental Sciences
University of Tsukuba
Tsukuba, Japan

benescu@geol.tsukuba.ac.jp
bogdan3j@gmail.com

Collaborators: Jim Mori, Masatoshi Miyazawa (Kyoto Univ.), Kazushige Obara (ERI), Shin Aoi, Tetsuya Takeda, Katsuhiko Shiomi, Kaoru Sawazaki (NIED), Sebastian Hainzl (GFZ), David Marsan (ISTerre), Zhigang Peng (Georgia Tech), Olivier Lengline (Strasbourg Univ.), Shinji Toda (Tohoku Univ.), Yehuda Ben-Zion (USC), Yuji Yagi, Kengo Shimojo, Ciaki Okada (Tsukuba Univ.)…

Main topics:

1) *Temporal features:*

- How the aftershocks rate decay immediately after the mainshock?
  - time domain;
  - energy domain;
- What this decay tells us about the aftershocks occurrence mechanism (rate-and-state friction law modeling)?

2) *Spatial features:*

- Migrations (indicating correlations with afterslip)?
- Correlations with the arrival of mainshock surface waves for remotely triggered events after Tohoku-oki earthquake (more than 1300 km from the mainshock)?
- Possible role of fluids in the activation of seismicity?

Early aftershocks - Time

Hi-net NIED

Hi-net（防災科学技術研究所高感度地震観測網）

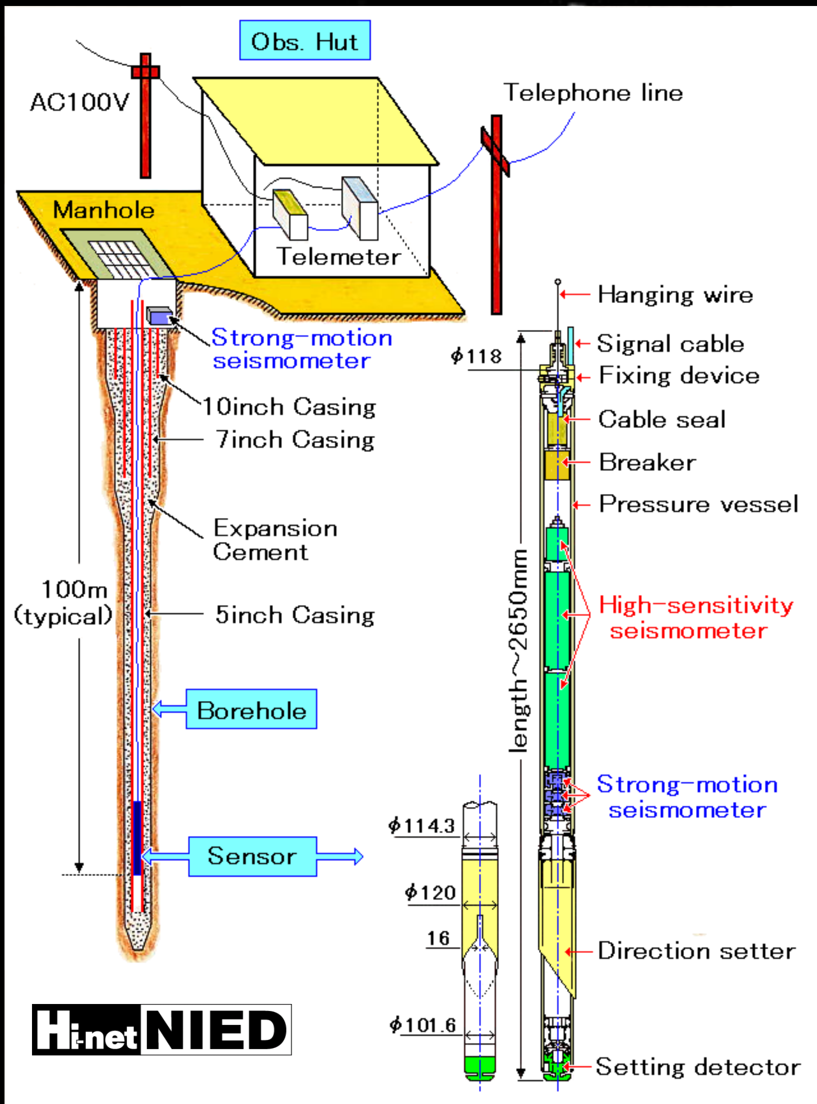

Courtesy of NIED

Early aftershocks - Time

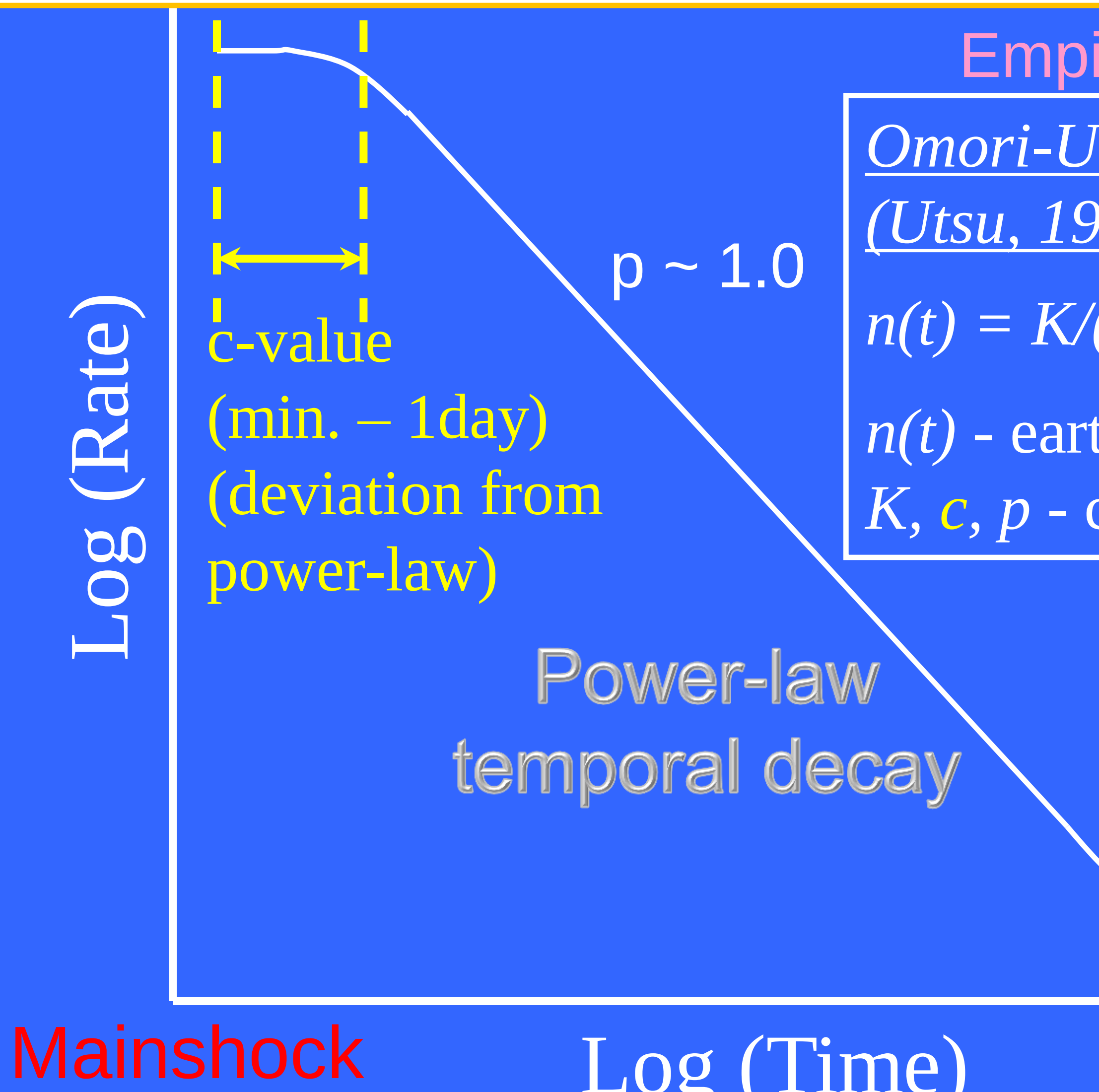

Aftershock rate versus time

Empirical law

Omori-Utsu law
(Utsu, 1961):

$n(t) = K/(t+c)^p$,

$n(t)$ - earthquake rate,
K, c, p - constants

大森房吉先生
(1868 – 1923)

Physics-based law

THE RATE AND STATE DEPENDENT FRICTION LAW PREDICTS DEVIATION FROM THE (POWER-LAW) OMORI LAW.

Early aftershocks - Time

THE BEGINNING OF AN AFTERSHOCK SEQUENCE :

1) *c-value* typically ranges from 0.5 to 20 hours (Utsu et. al., 1995);

2) Kagan (2004): INCOMPLETENESS prohibits assessing early aftershocks from catalogs, but probably *c-value* (of the Omori-Utsu law) is 0;

3) *c-value* is LARGER THAN 0 and depends on the MINIMUM MAGNITUDE (Shcherbakov et al., 2004; Nanjo et al., 2007);

4) Peng et al. (2006, 2007) and Enescu et al. (2007, 2009): *c-values* of less than A FEW MINUTES from the study of high- resolution waveform data from Japan and US;

Early aftershocks - Time

Two main techniques are used to detect earthquakes "hidden" within the noisy waveforms:

1) Simply quantifying (counting + magnitude determination) the seismic events revealed by high-pass filtering of seismic waveforms [e.g., Peng et al., 2007; Enescu et al., 2007; Marsan and Enescu , 2012]. No location available. Sometimes the envelopes are used instead of the high-pass filtered waveforms.

2) A second technique is based on the correlation of the continuous seismic signal with pre-determined template events. This technique has been initially applied to detect low frequency earthquakes (LFE) [Shelly et al., 2007]. It has also been proven successful in recovering missing earthquakes during aftershock [Peng & Zhao, 2009; Enescu et al., 2010; Kato et al., 2012; Lengline et al., 2012], foreshock [Bouchon et al., 2011] and remotely triggered earthquake sequences [Meng et al., 2012].

Early aftershocks - Time

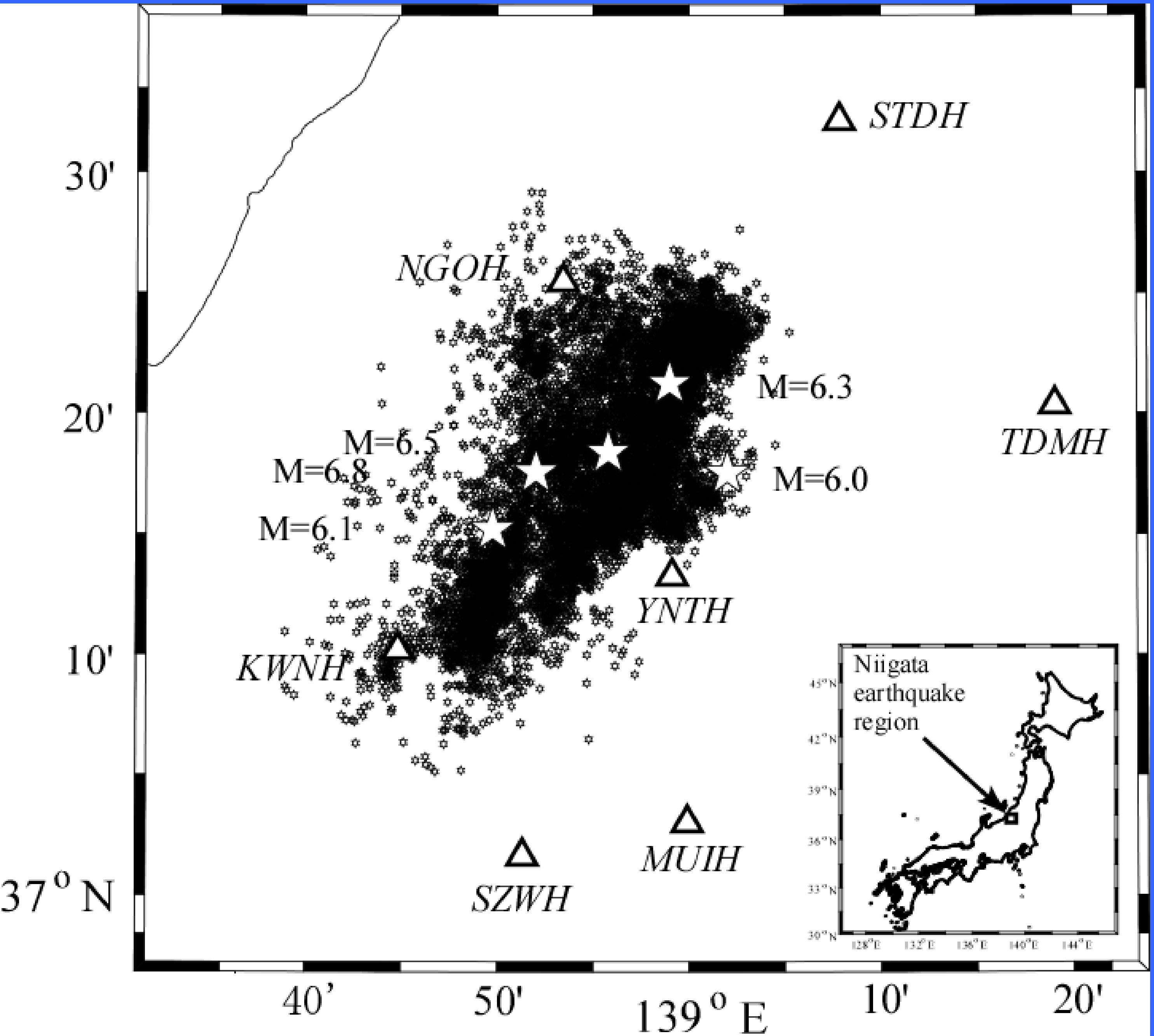

Large events:

Mainshock:
M6.8: 10/23, 17:56

Aftershocks:
M6.3, 18:03
M6.0: 18:11
M6.5: 18:34
M6.1: 10/27, 10:40

Enescu, Mori, Miyazawa, JGR, 2007

Data processing:

1. High-pass filter the waveform data to detect small events hidden in the low-frequency coda.

2. The magnitude is calibrated using a set of events that are both detected on seismograms and listed in the JMA catalog.

3. Combine the waveform based catalog with the JMA catalog.

4. Analyse the aftershock decay of the combined catalog (Omori-Utsu law + maximum likelihood method, Ogata, 1983).

Early aftershocks - Time

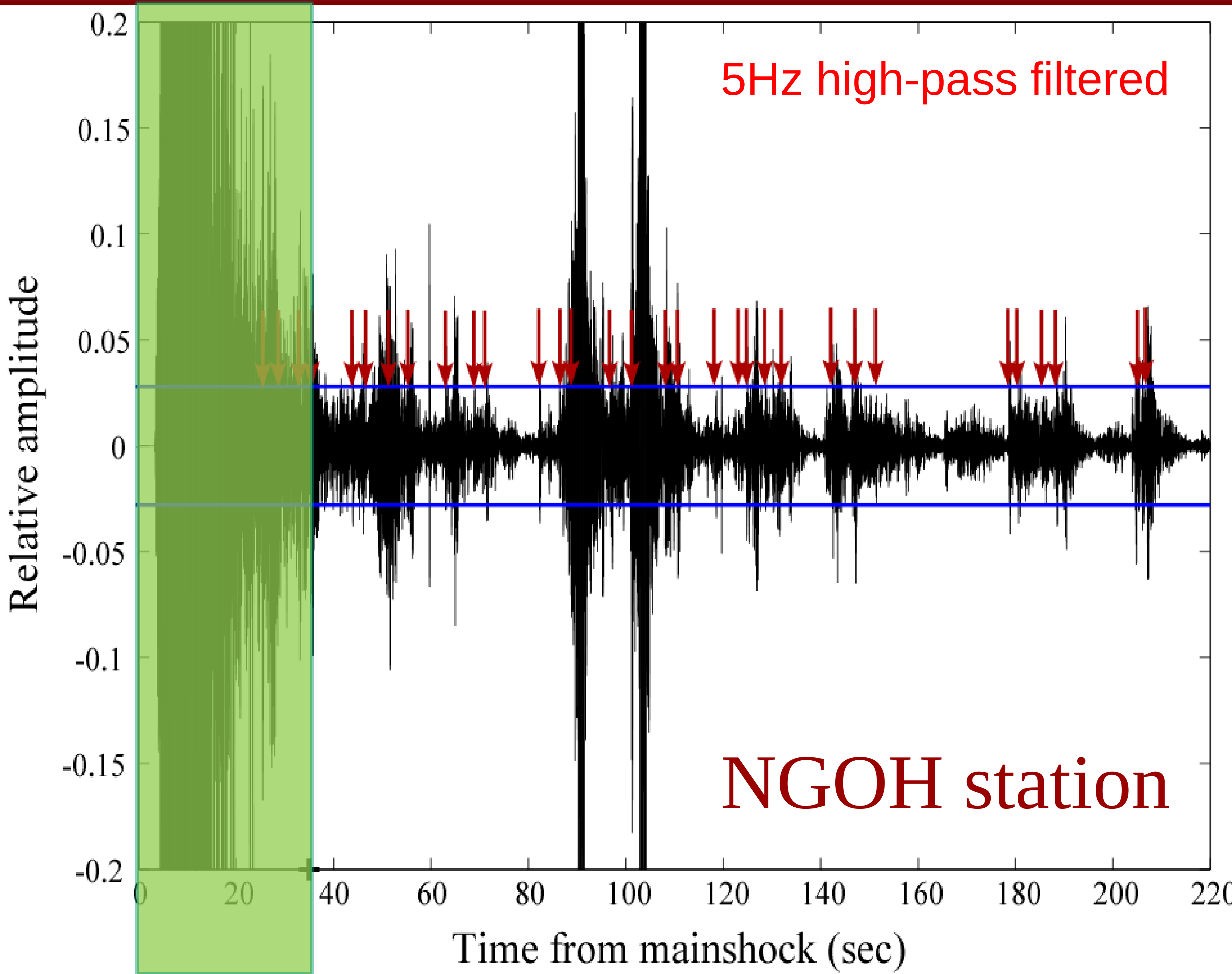

Enescu et al., JGR, 2007

Early aftershocks - Time

c-value ~ 4 minutes

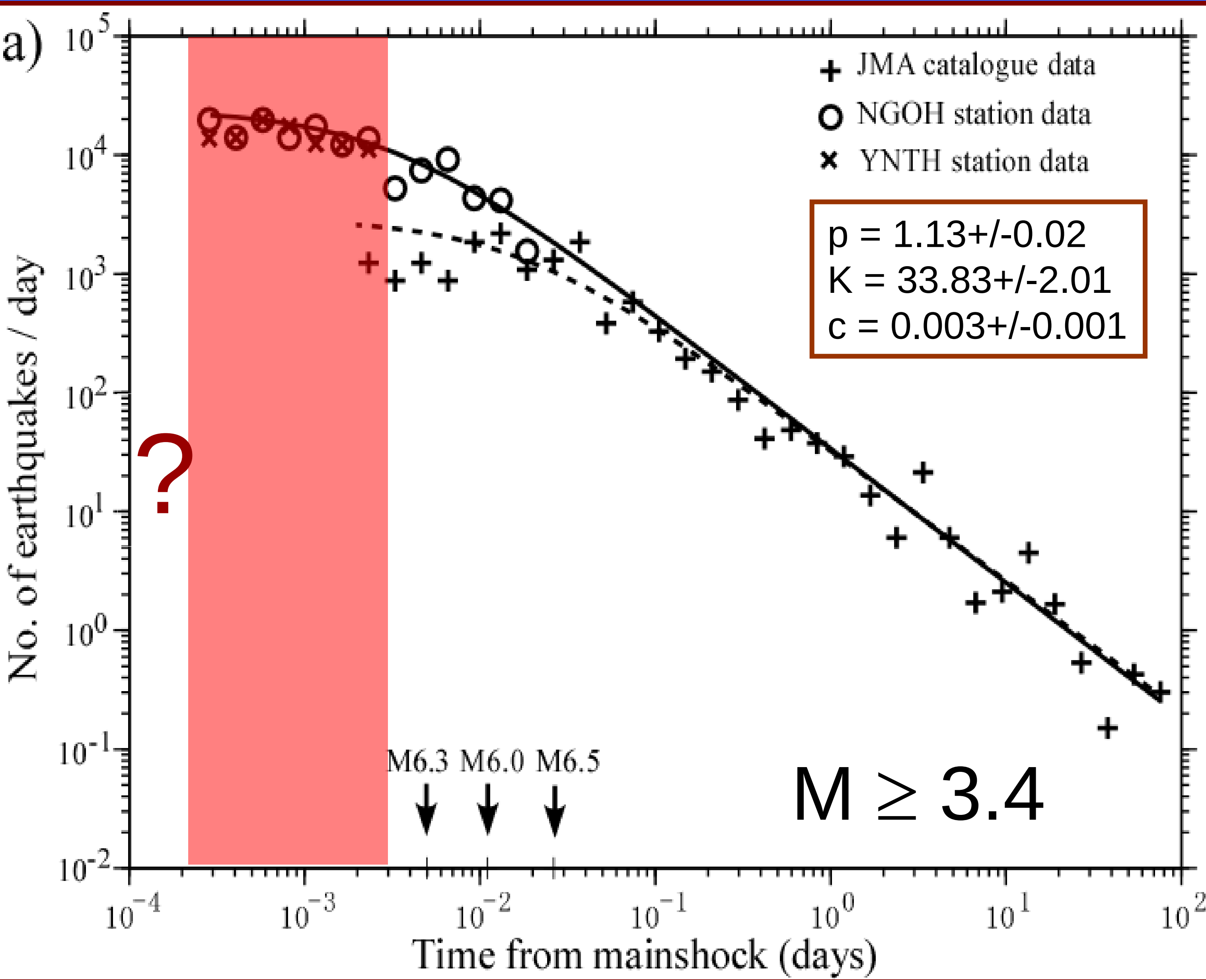

There are fewer aftershocks than predicted by the Omori law in the first 0.003 days after the mainshock.

Time decay of the number of aftershocks, picked from seismograms at Ngoh (o), Ynth stations (x) and JMA (+).

Enescu et al., JGR, 2007

Early aftershocks - Time

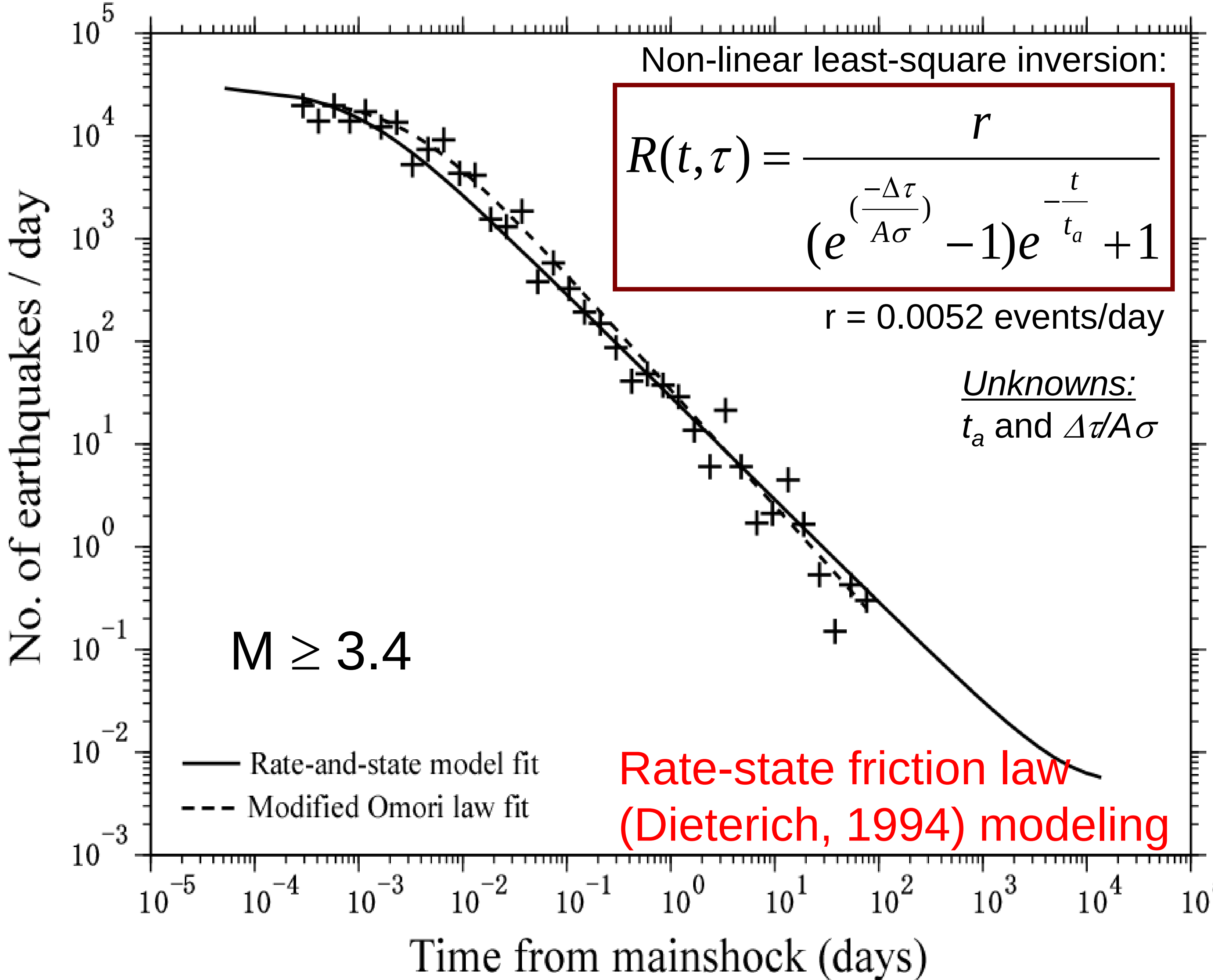

$$R(t,\tau) = \frac{r}{\left(e^{\left(\frac{-\Delta\tau}{A\sigma}\right)} - 1\right) e^{-\frac{t}{t_a}} + 1}$$

Rate-state friction law (Dieterich, 1994) modeling

Enescu et al., JGR, 2007

Early aftershocks - Time

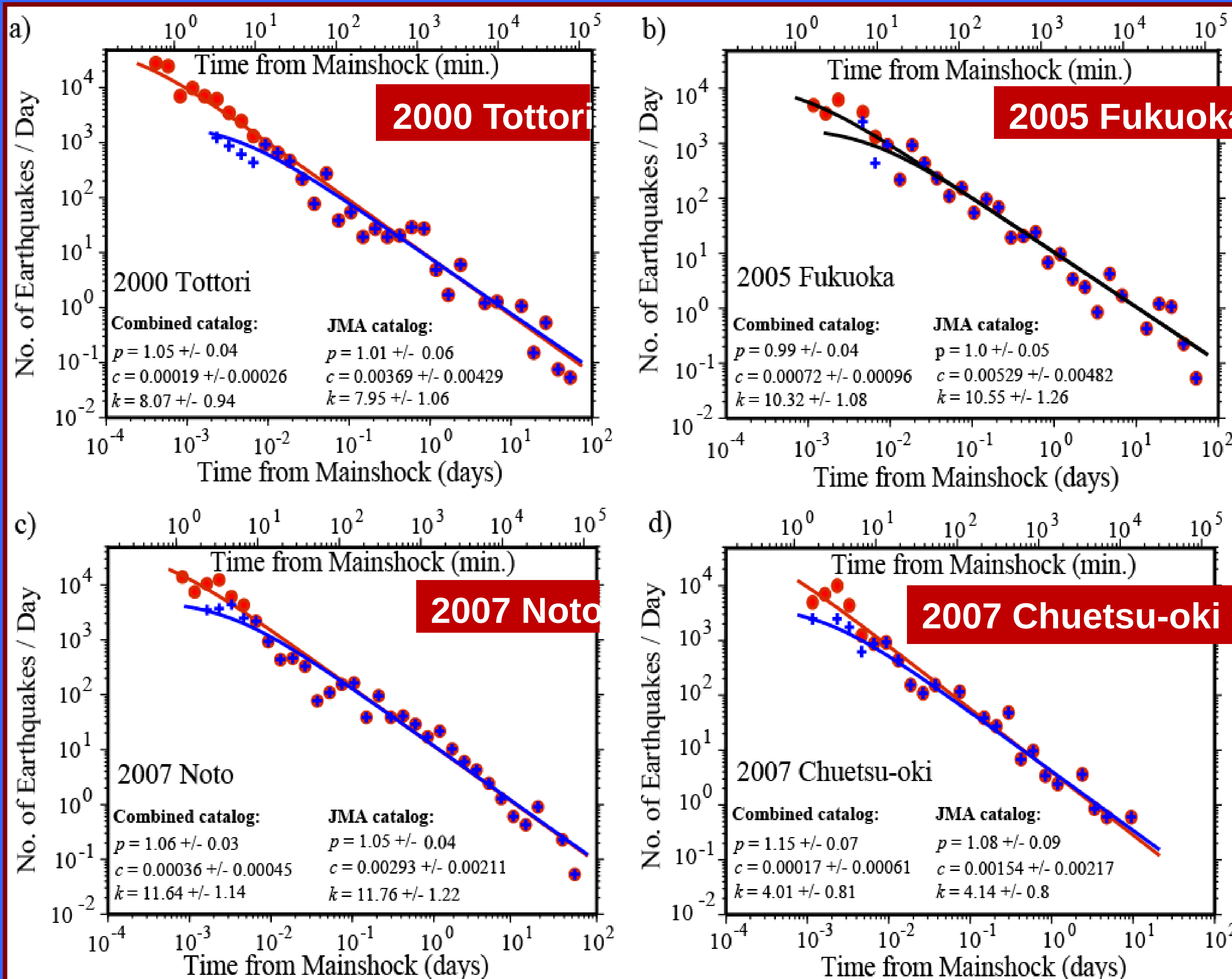

M ≥ 3.5

c-value ~ less than a few minutes

Enescu et al., BSSA, 2009

Working in the energy domain

Synthesis of seismic wave envelope

Incoherent propagation of high-freq. seismic waves

$$E \approx W * P * S$$

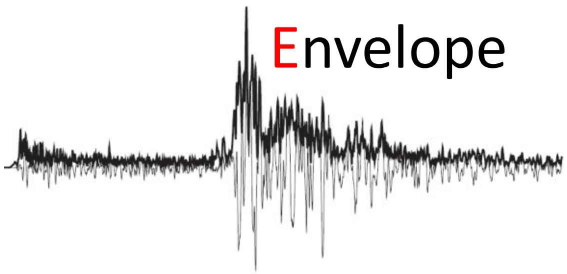

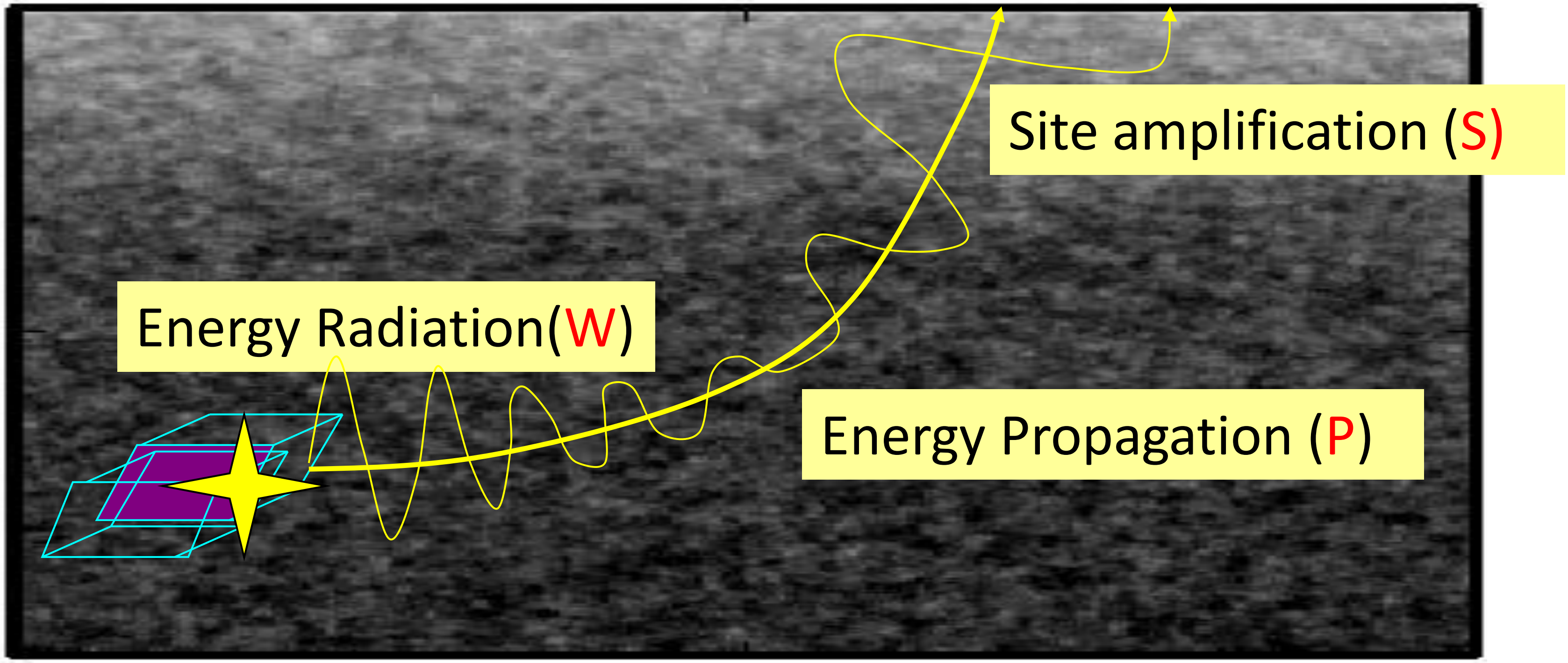

Sawazaki and Enescu, JGR, 2013

Energy propagation process

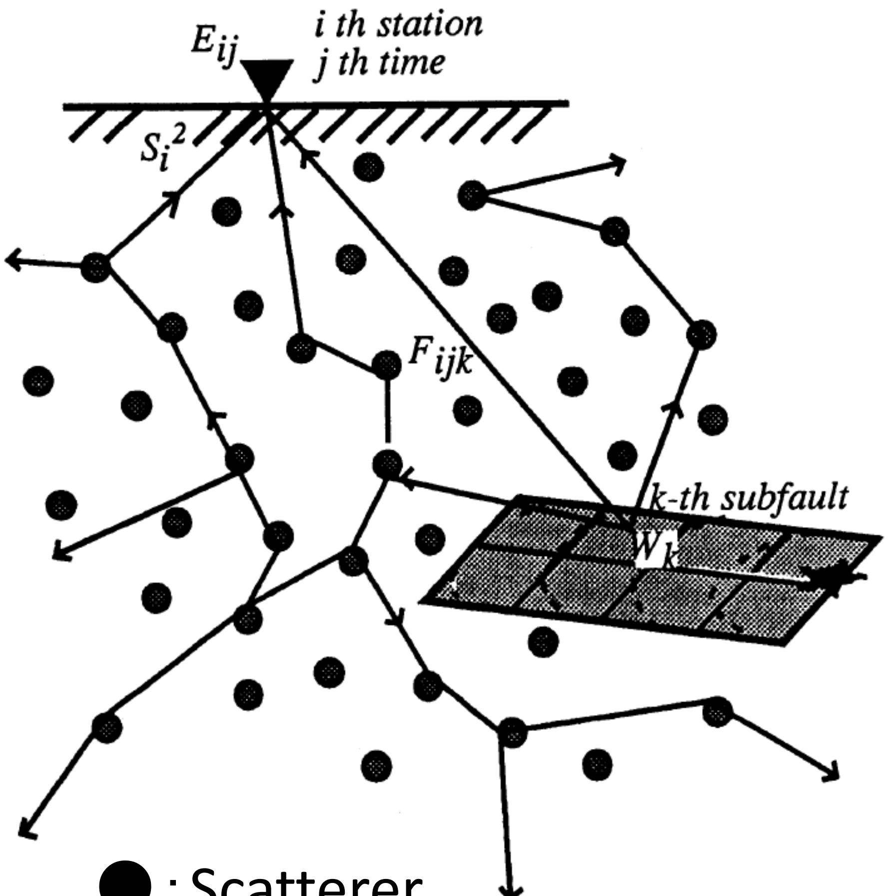

● : Scatterer

→ : Energy path

Nakahara et al. (1998)

$$P(R, f, t) \approx \frac{\exp\left[-\left(g_0(f)V_0 + 2\pi Q^{-1}(f) f\right)t\right]}{4\pi V_S R^2}\delta\left(t - \frac{R}{V_S}\right) +$$

$$\frac{\left[1 - R^2/(V_S t)^2\right]^{1/8}}{\left[4\pi V_S t/(3 g_0(f))\right]^{3/2}} \exp\left\{-\left[g_0(f)V_S + 2\pi Q^{-1}(f) f\right]t\right\} \times$$

$$M\left[g_0(f)V_0 t\left(1 - \frac{R^2}{V_S^2 t^2}\right)^{3/4}\right] H\left(t - \frac{R}{V_S}\right)$$

$$M(x) \equiv \exp(x)\sqrt{1 + 2.026/x}$$

R: Source distance

V_S=3.5km/s (fixed)

$g_0(f)$: scattering coefficient

$Q^{-1}(f)$: inverse intrinsic Q-factor

To account for the multiple scattering of S wave energy for a point-like impulsive source, we use the equation proposed by Paasschens [1997] as the envelope Green's function P.

Sawazaki and Enescu, JGR, 2013

Synthesized envelope

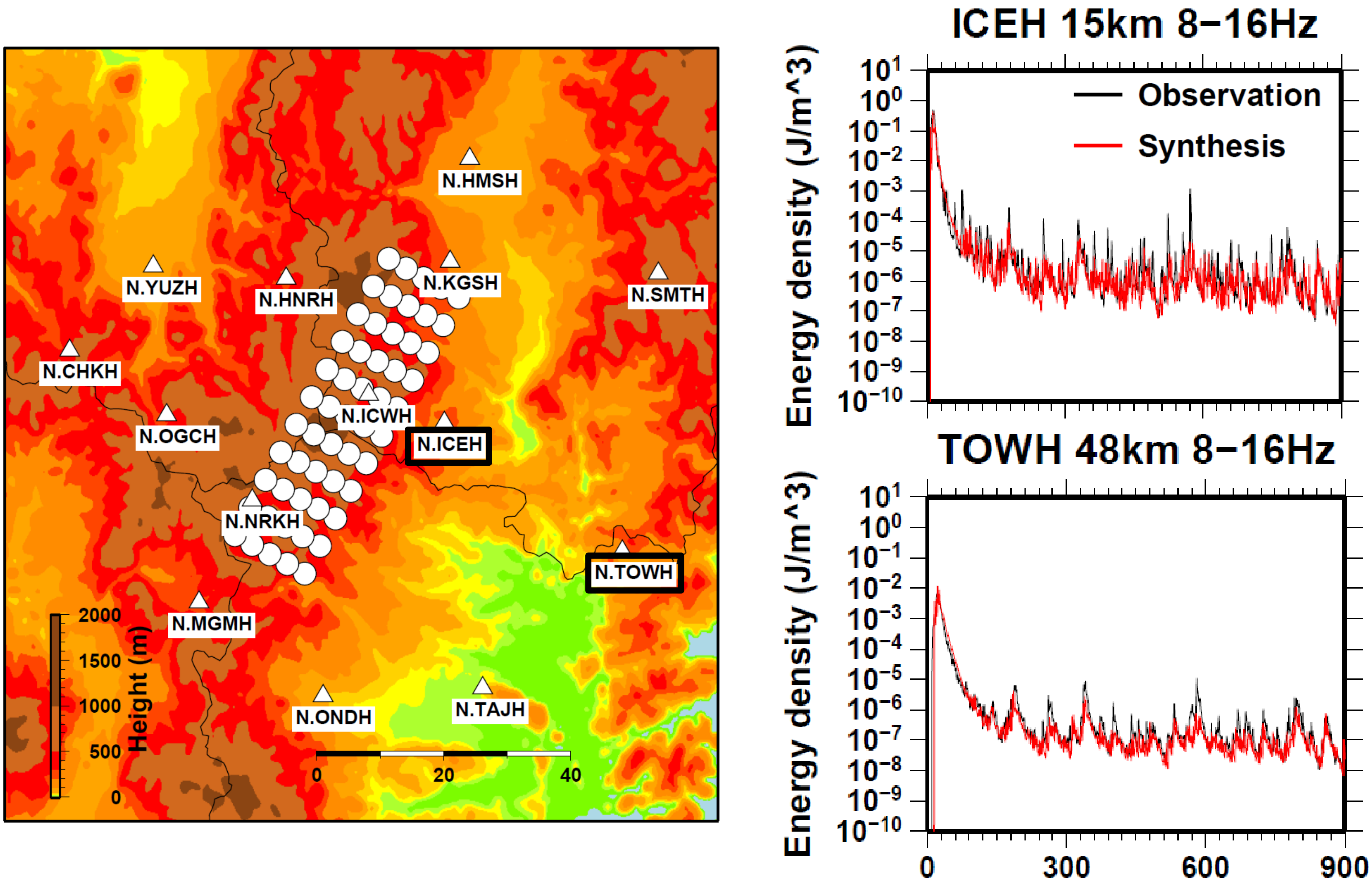

Sawazaki and Enescu, JGR, 2013

Energy release rate

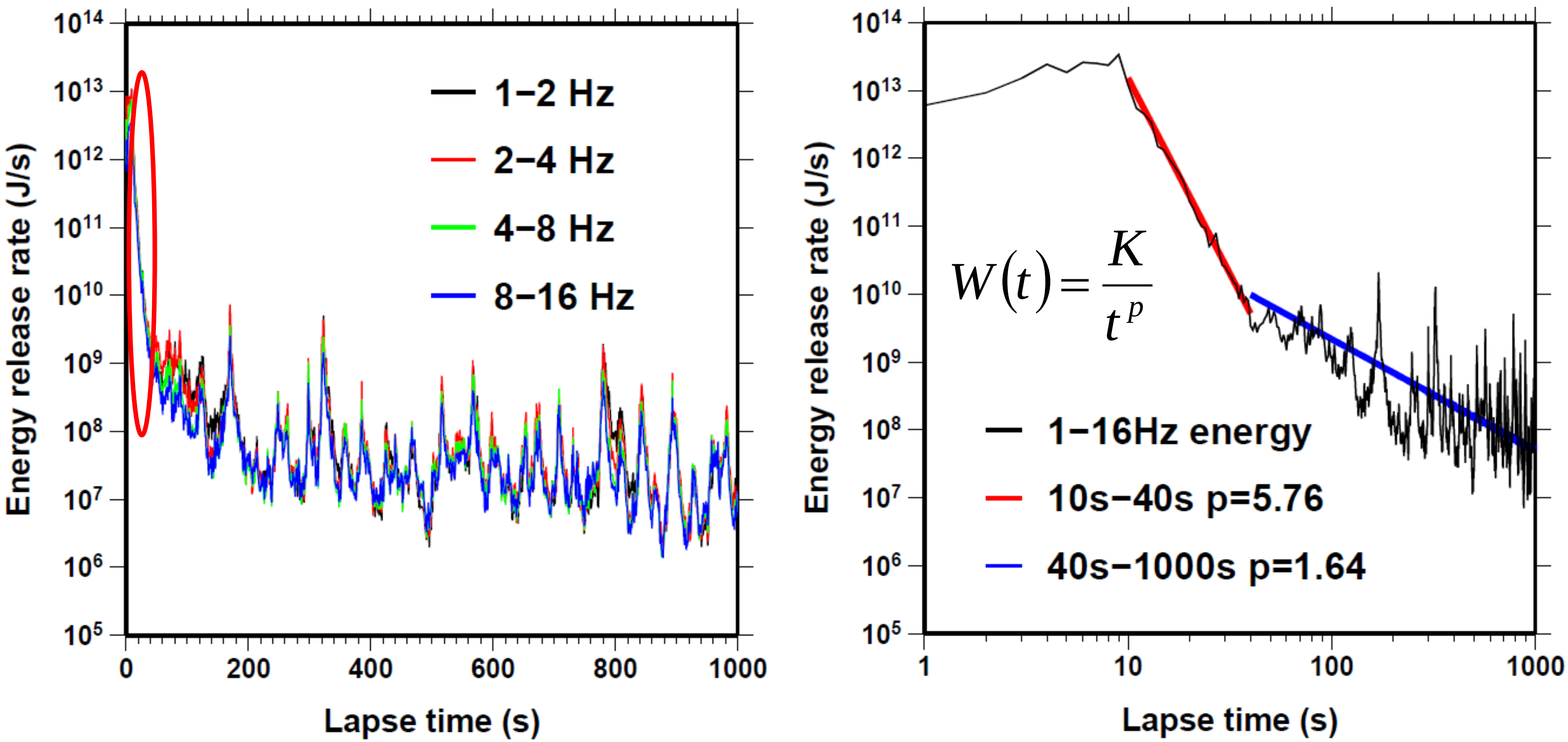

Energy radiation function shows a slope of 1.6 for times larger than ∼ 40s.

Sawazaki and Enescu, JGR, 2013

Early aftershocks - Time

Why c-values are very small?

According to the rate-and-state friction law:

$$n(t) = \frac{K}{t + c}$$

$$K = \left(\frac{A\sigma}{\dot{\tau}}\right) r$$

$$c = \left(\frac{A\sigma}{\dot{\tau}}\right) \exp\left(\frac{-\Delta CFS}{A\sigma}\right)$$

n(t) – aftershock frequency
K – productivity
c – delay-time

A – dimensionless fault constant parameter
σ – normal stress
$\dot{\tau}$ – tectonic stressing rate

Large values of stress change result in small c-values:
➔ *high stress heterogeneity can explain small c-values*

Early aftershocks - Space

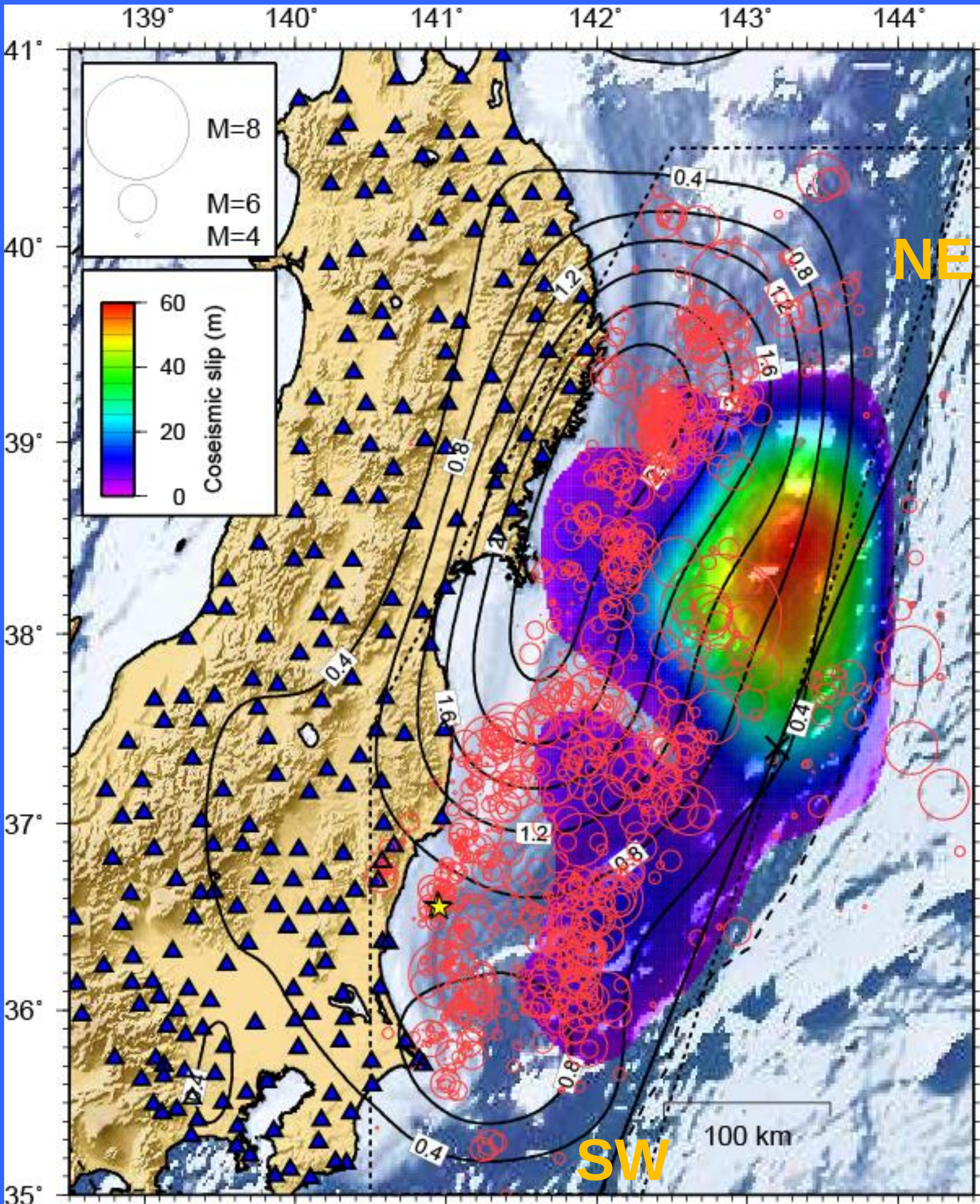

Decay and expansion of the early aftershock activity, following the 2011, Mw9.0 Tohoku earthquake

Lengline, Enescu, Peng & Shiomi, GRL, 2012

Distribution of Hi-net catalog aftershocks occurred in the first eight days from the Tohoku-oki mainshock (red circles), slip (colored) and afterslip distribution (Ozawa et al., Nature, 2011)

Early aftershocks - Space

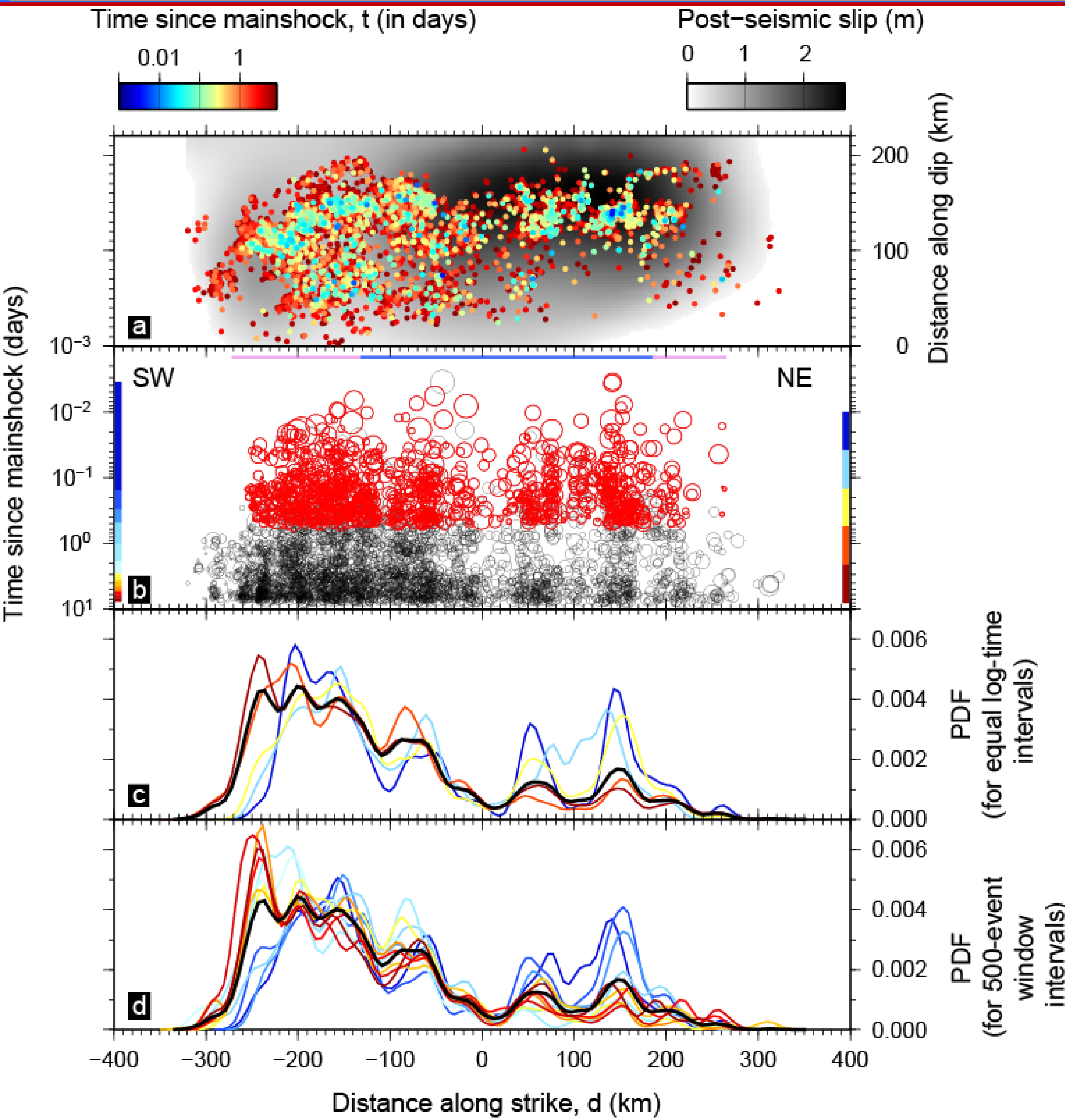

2011 Tohoku-oki earthquake (M9.0):

Aftershock area expansion

Lengline, Enescu, Peng & Shiomi, *GRL*, 2012

Early aftershocks - Space

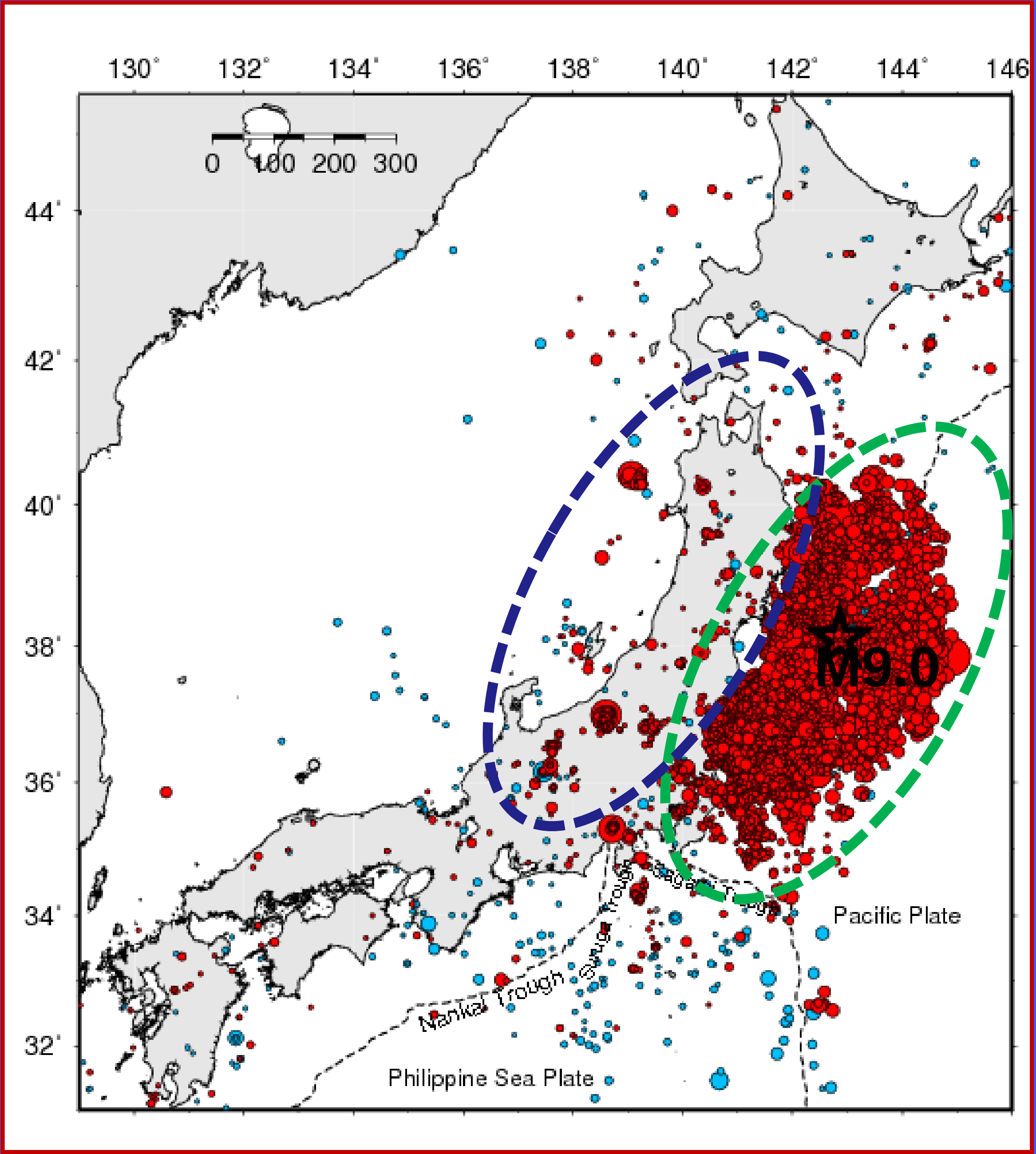

JMA catalog:

- one month before Tohoku eq.

- one month after Tohoku eq.

M ≥ 2.5

Clear activation of inland seismicity (Toda et al., 2011, Hirose et al., 2011, Enescu et al., 2011)

Early aftershocks – Time and Space

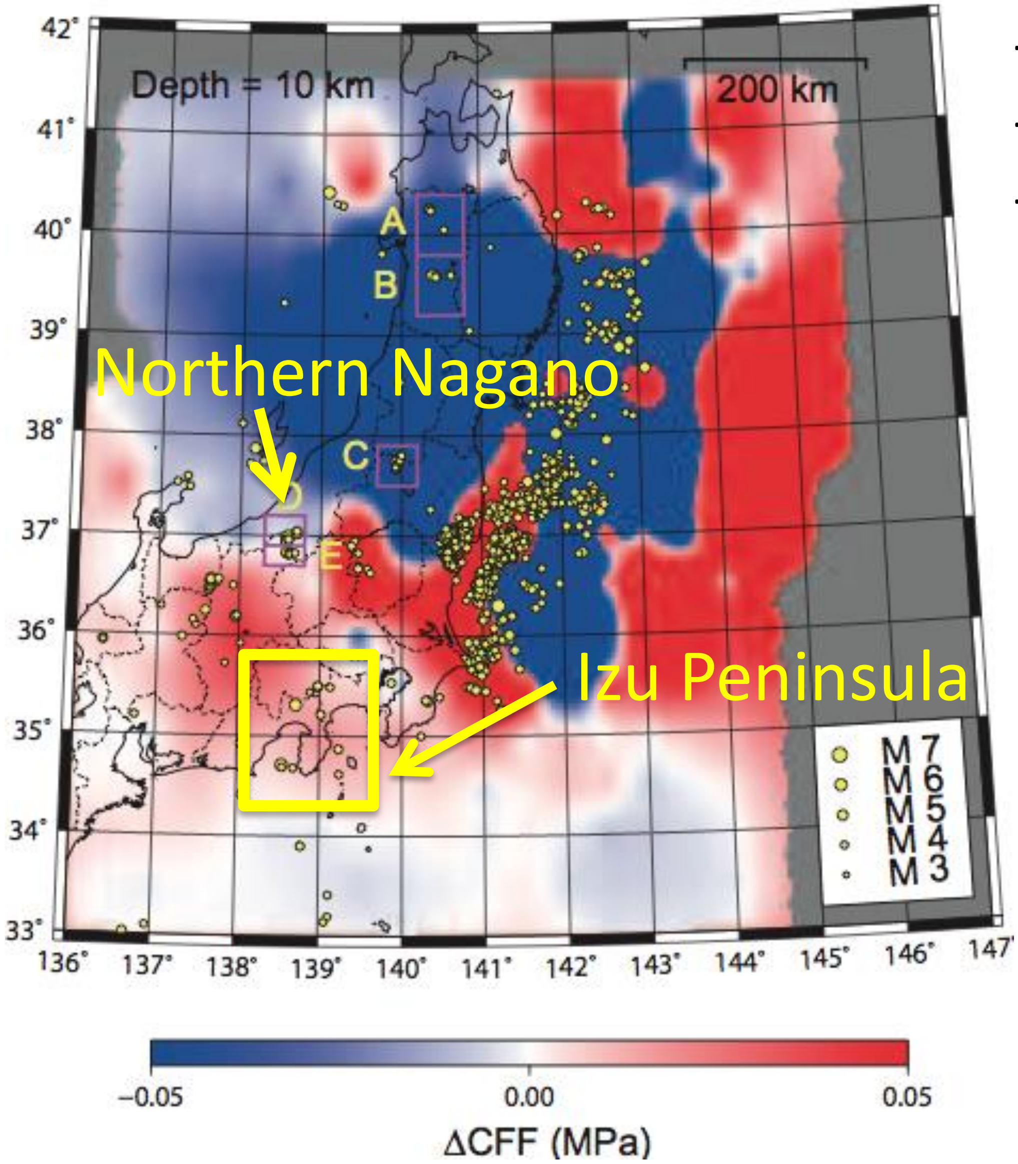

- Heterogeneous stress regime
- Geothermal/fluid-rich areas
- Dynamic triggering

Static stress changes resolved on the predominant seismogenic structures

Terakawa et al.(2013)

Static stress triggering near Izu Peninsula

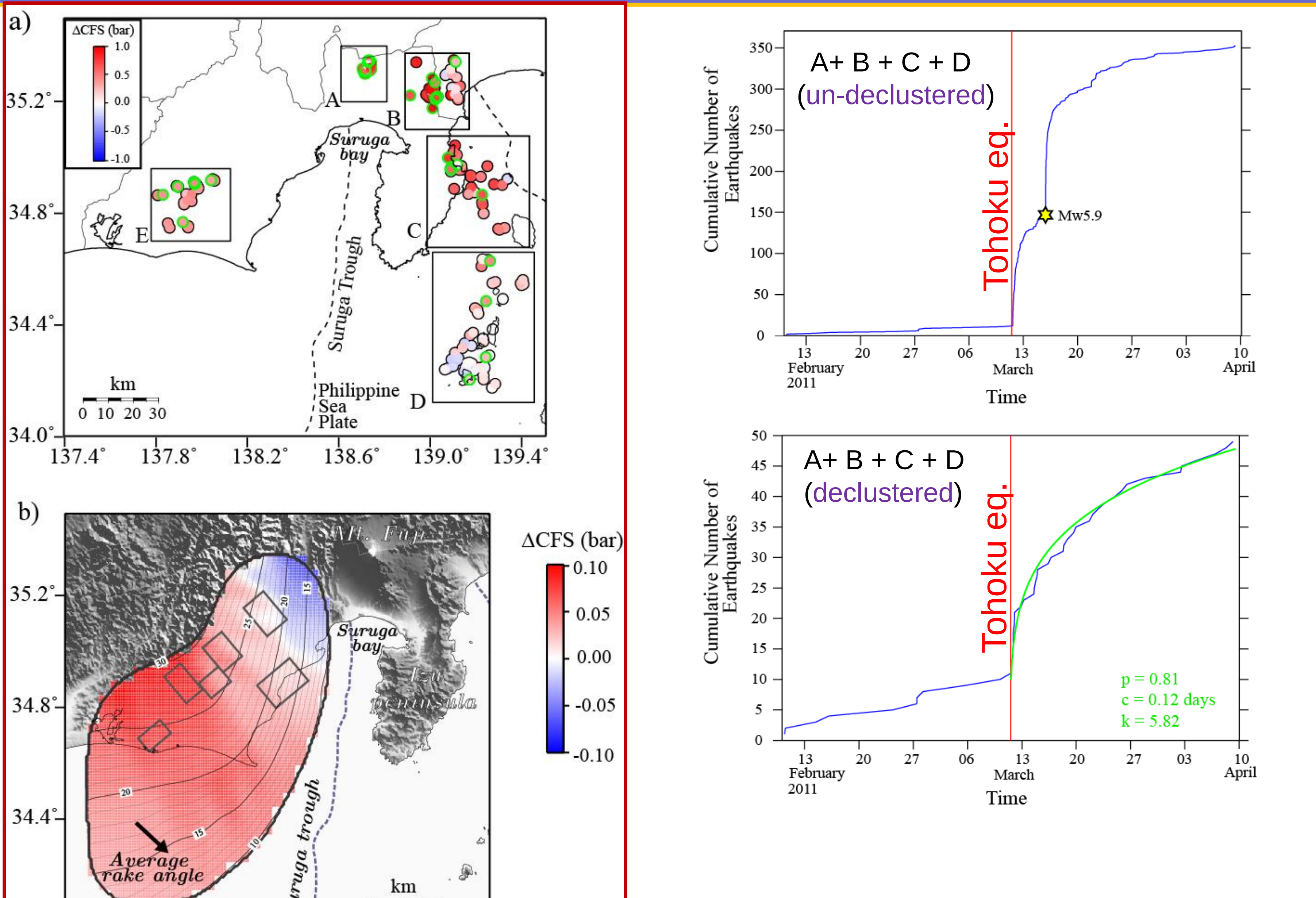

Enescu, Aoi, Toda et al., GRL, 2012

Early aftershocks – Time and Space

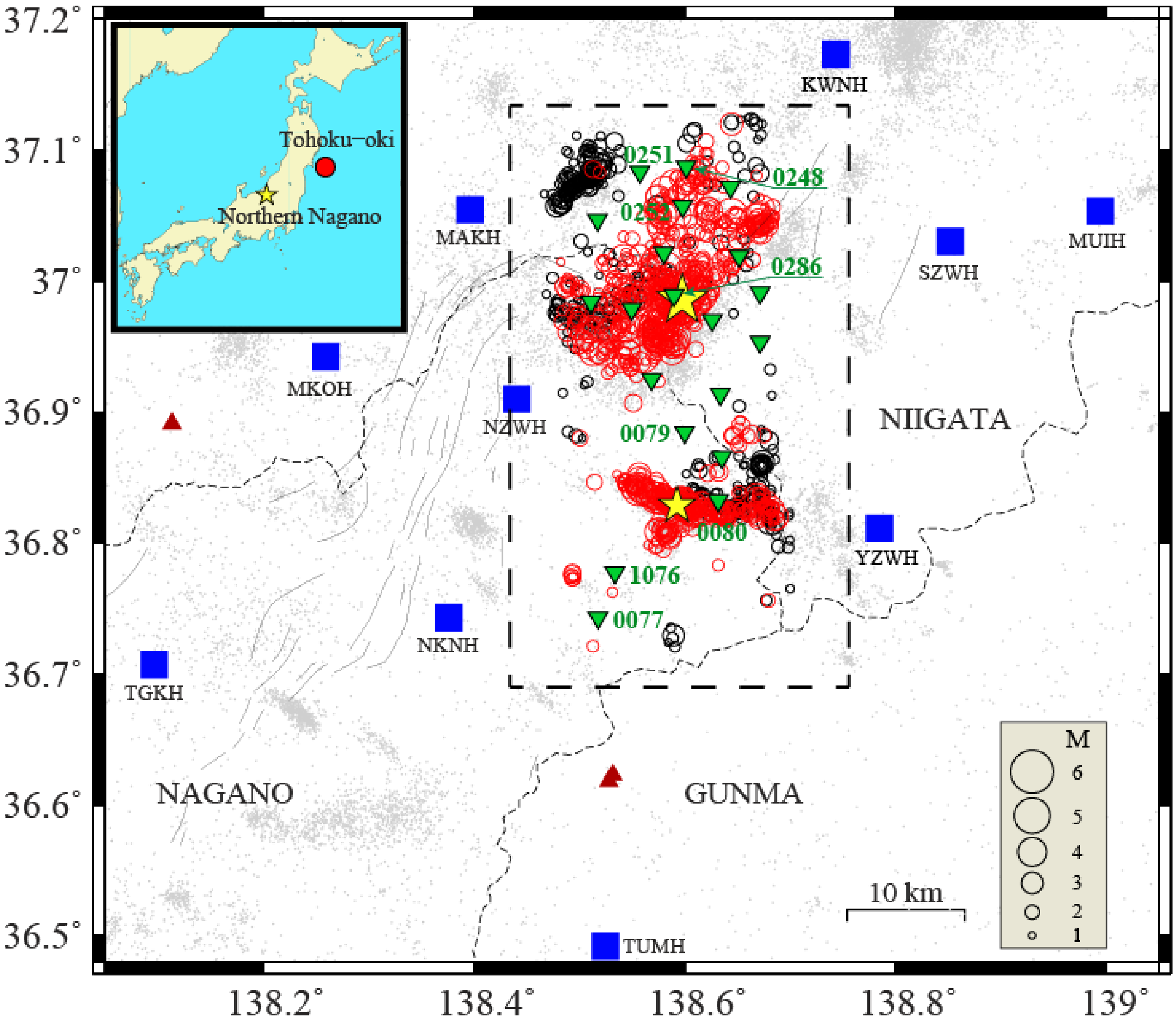

2011 M6.2 Nagano earthquake sequence

Shimojo, Enescu, Yagi & Takeda, GRL, 2014

Early aftershocks – Time and Space

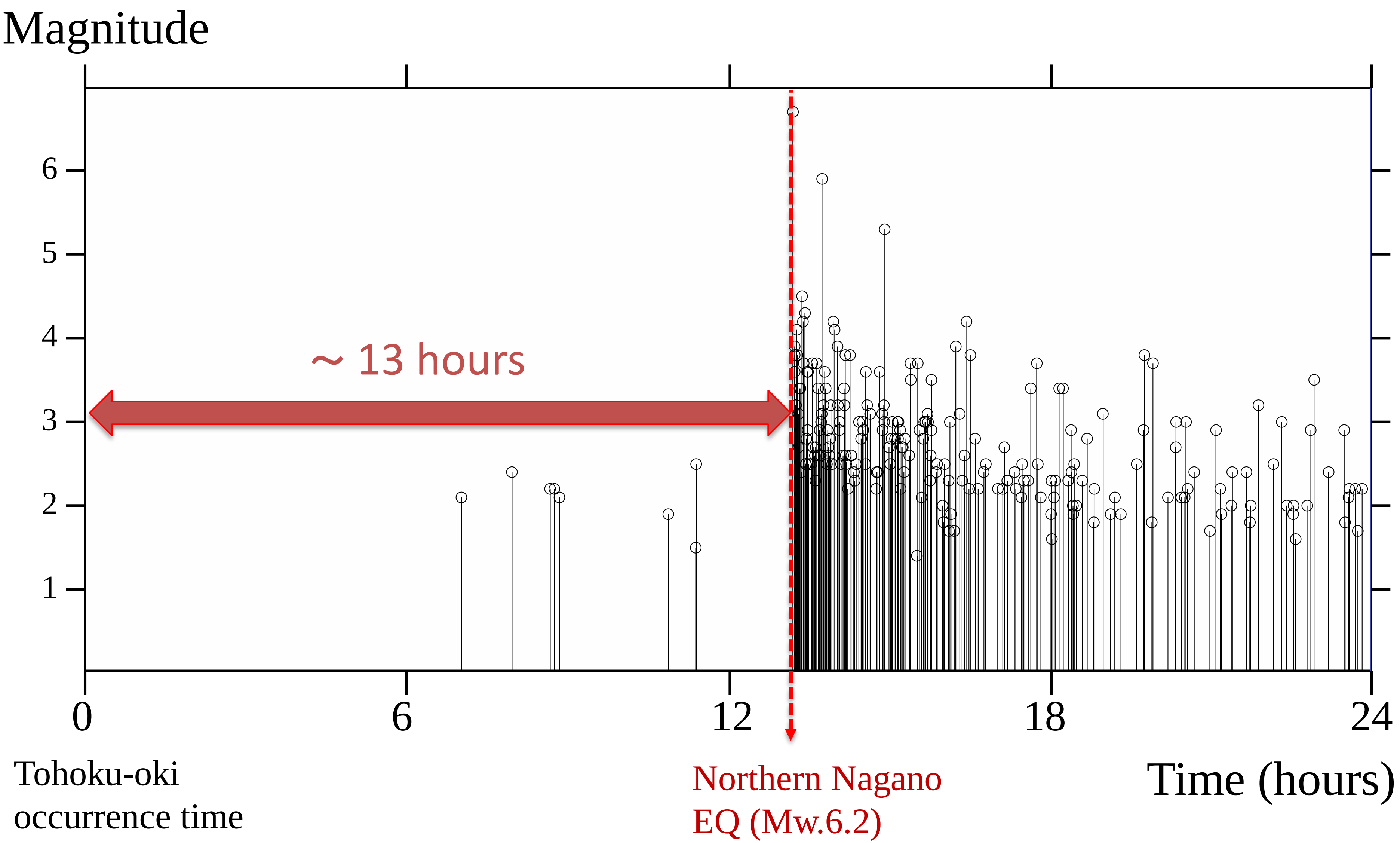

Time distribution of events in northern Nagano region

Early aftershocks – Time and Space

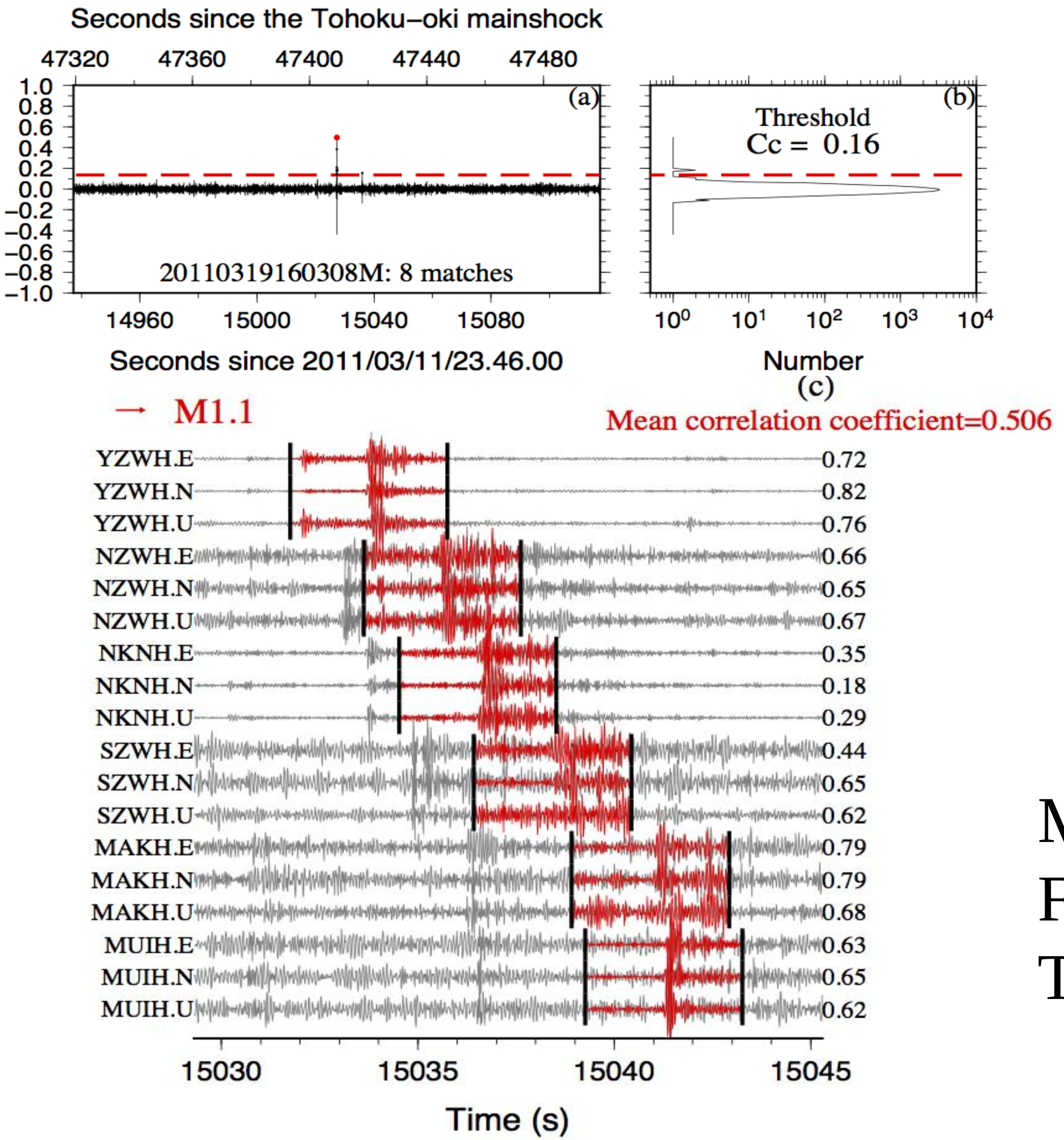

Matched Filter Technique

Early aftershocks – Time and Space

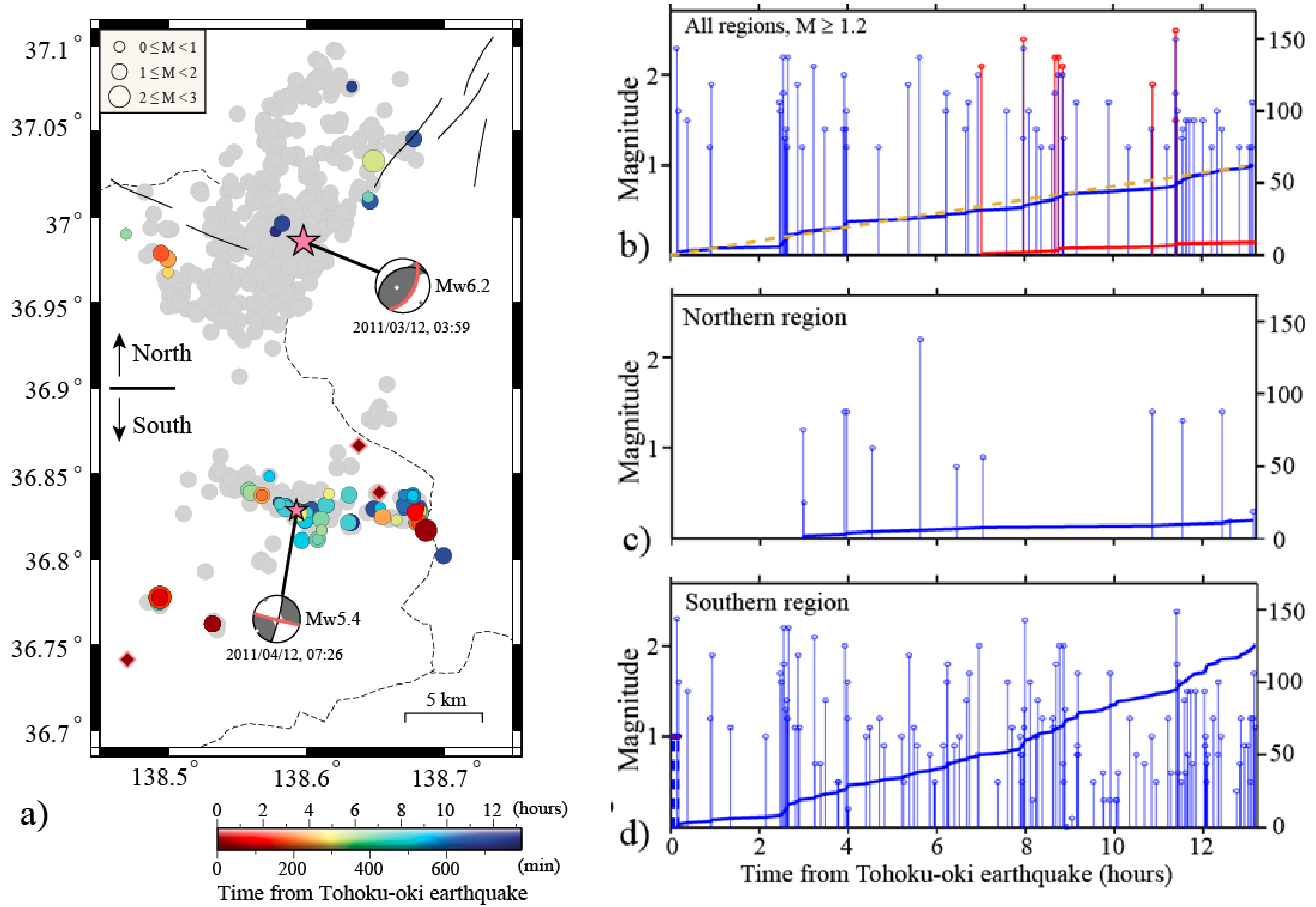

Early aftershocks – Time and Space

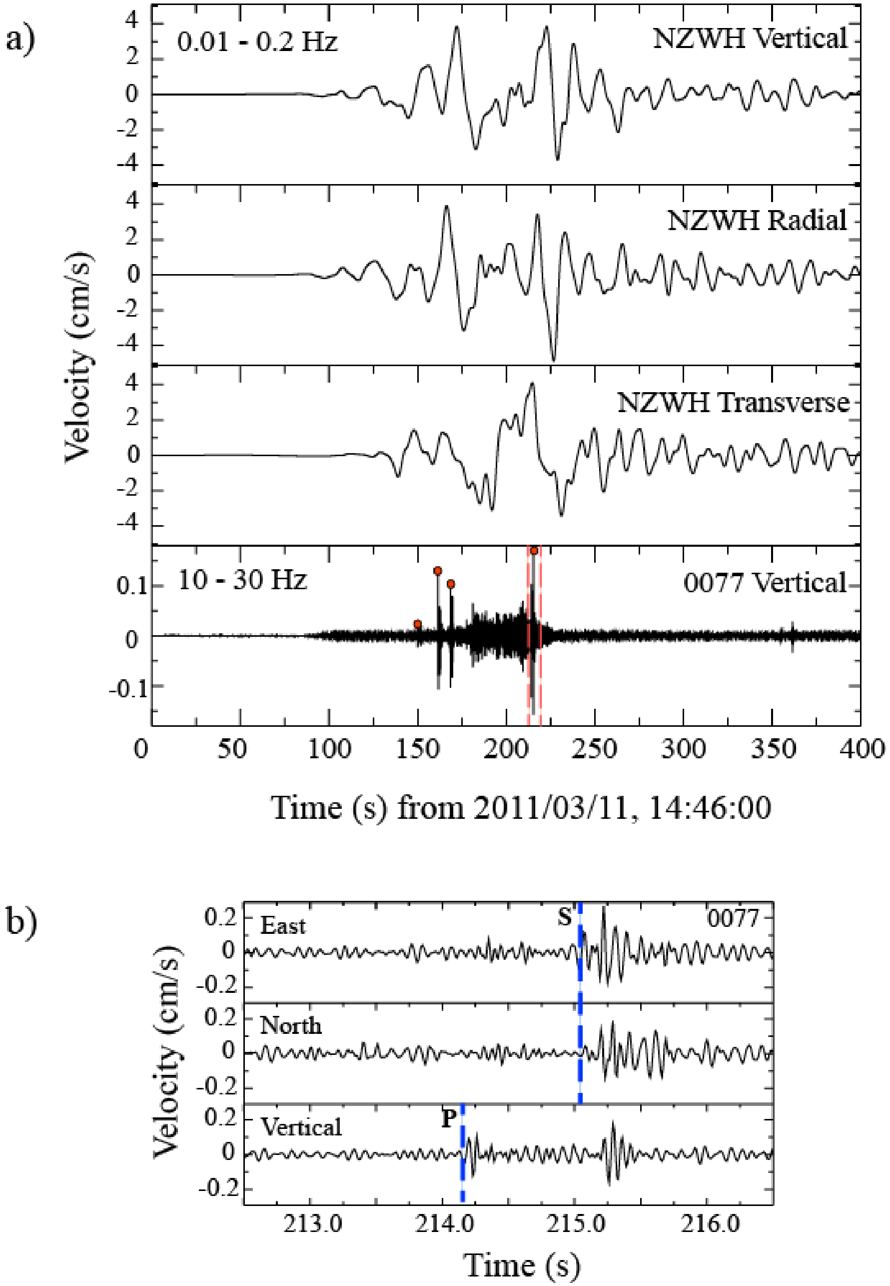

Dynamic triggering at the arrival of surface waves

Early aftershocks – Time and Space

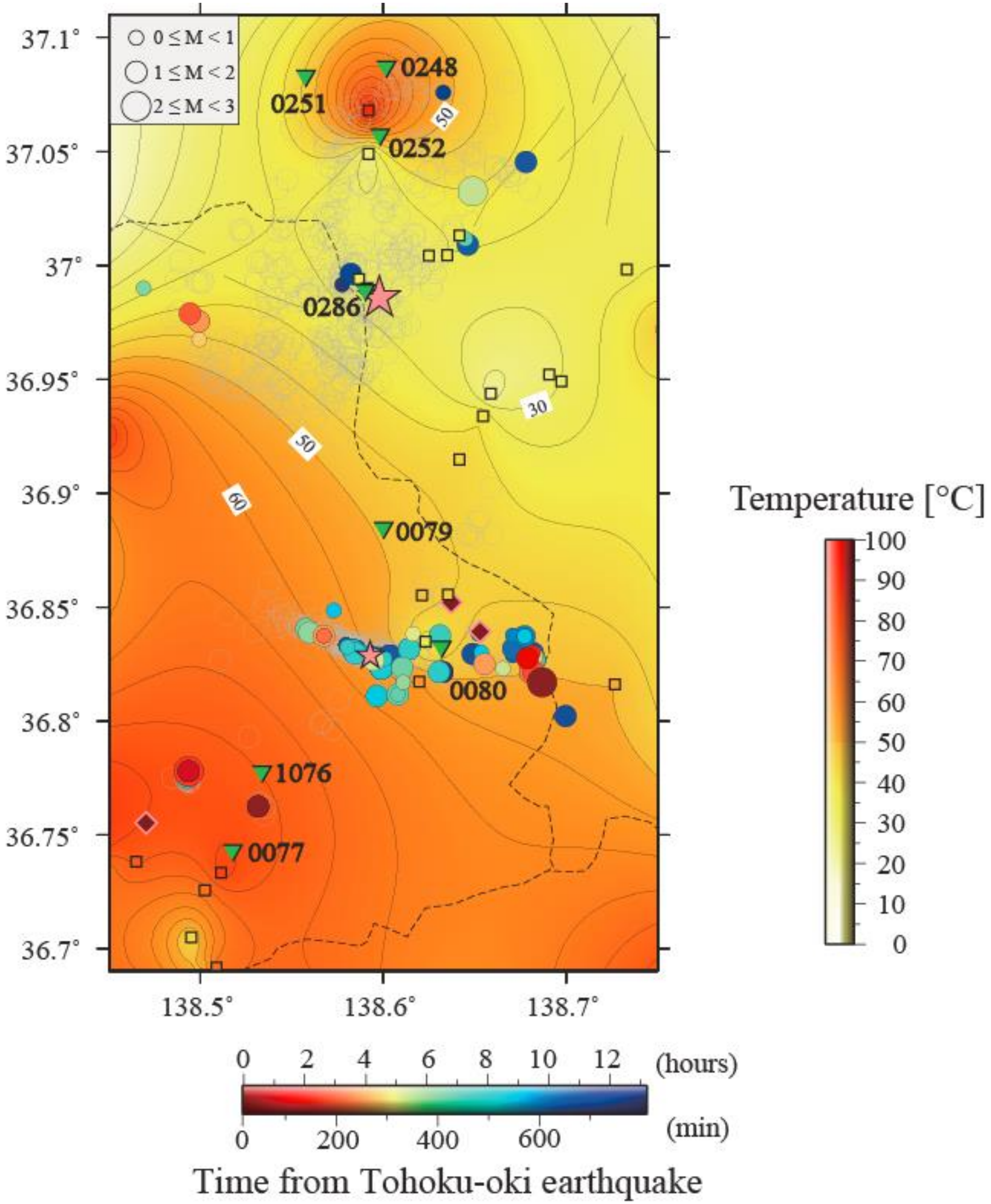

Higher fluid temperature and fluid flux in the "South"

Geothermal map of study area, with seismicity superposed. Temperature distribution was obtained by smoothly interpolating locally measured values from locations of small rectangles available all-over Japan

Early aftershocks – Time and Space

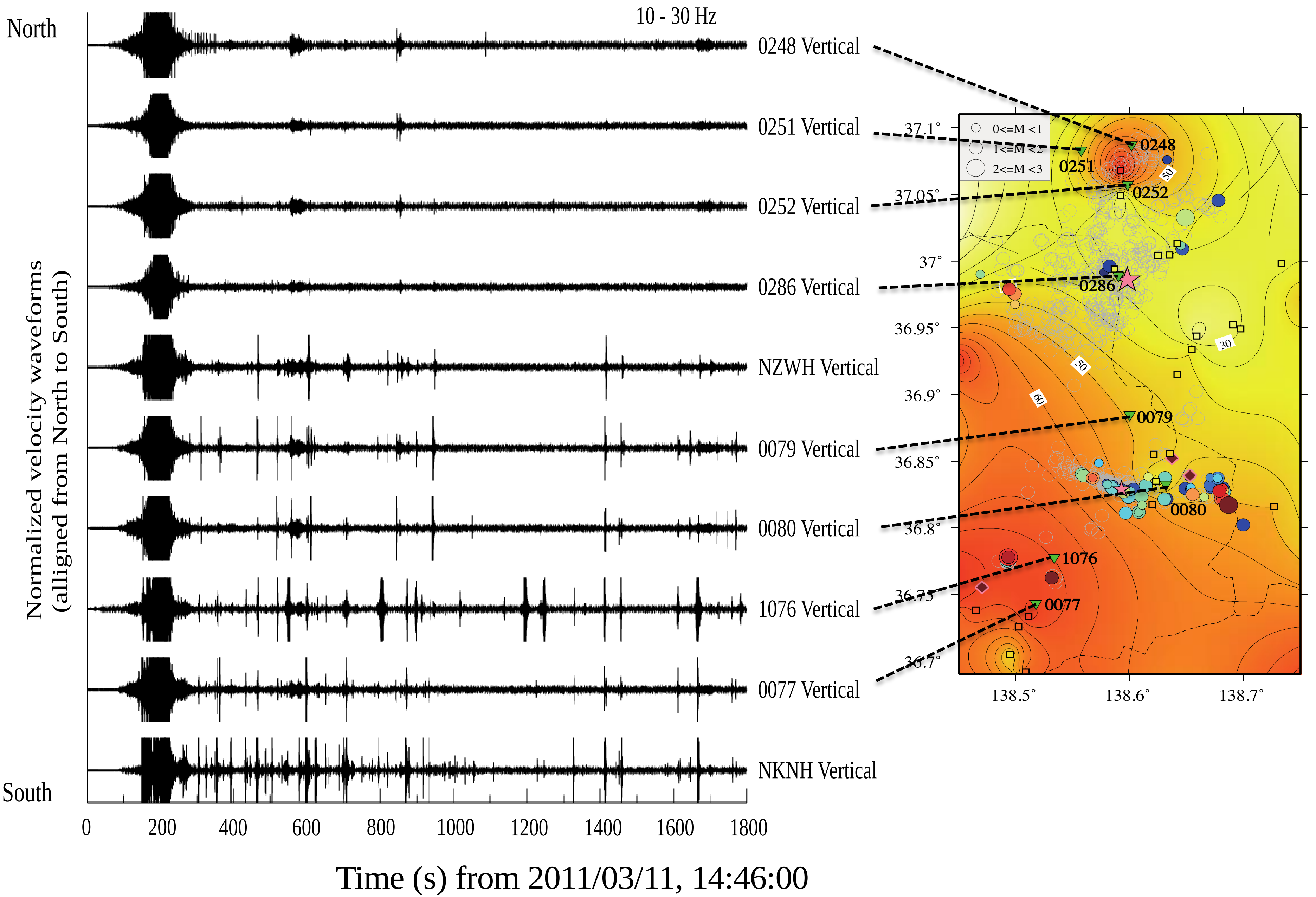

Early aftershocks – Time and Space

Large Vp/Vs at depth, probable existence of a deep fluid reservoir.

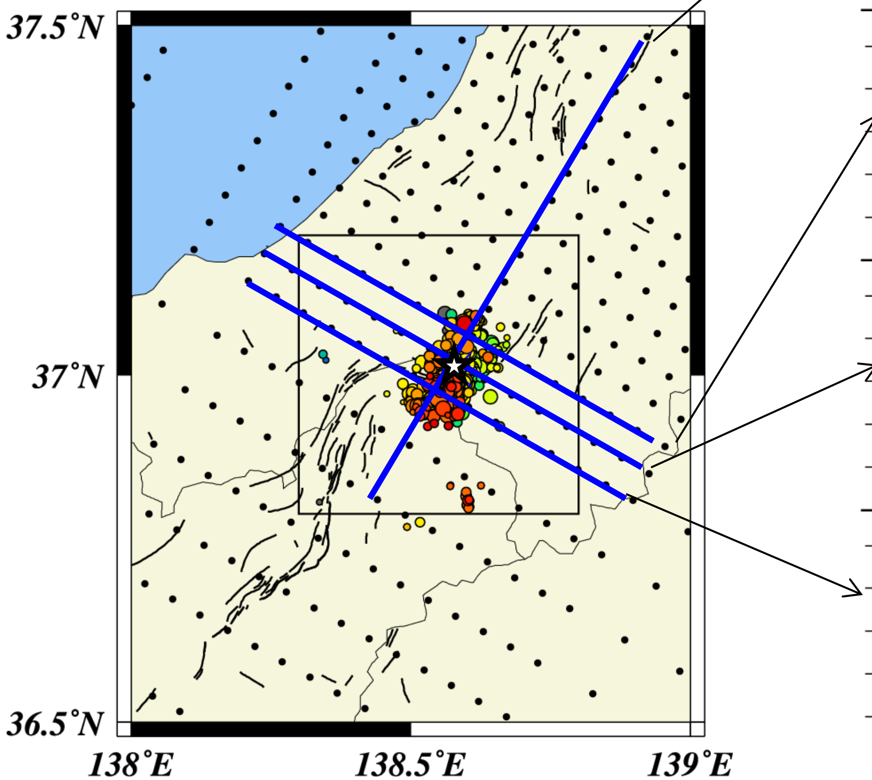

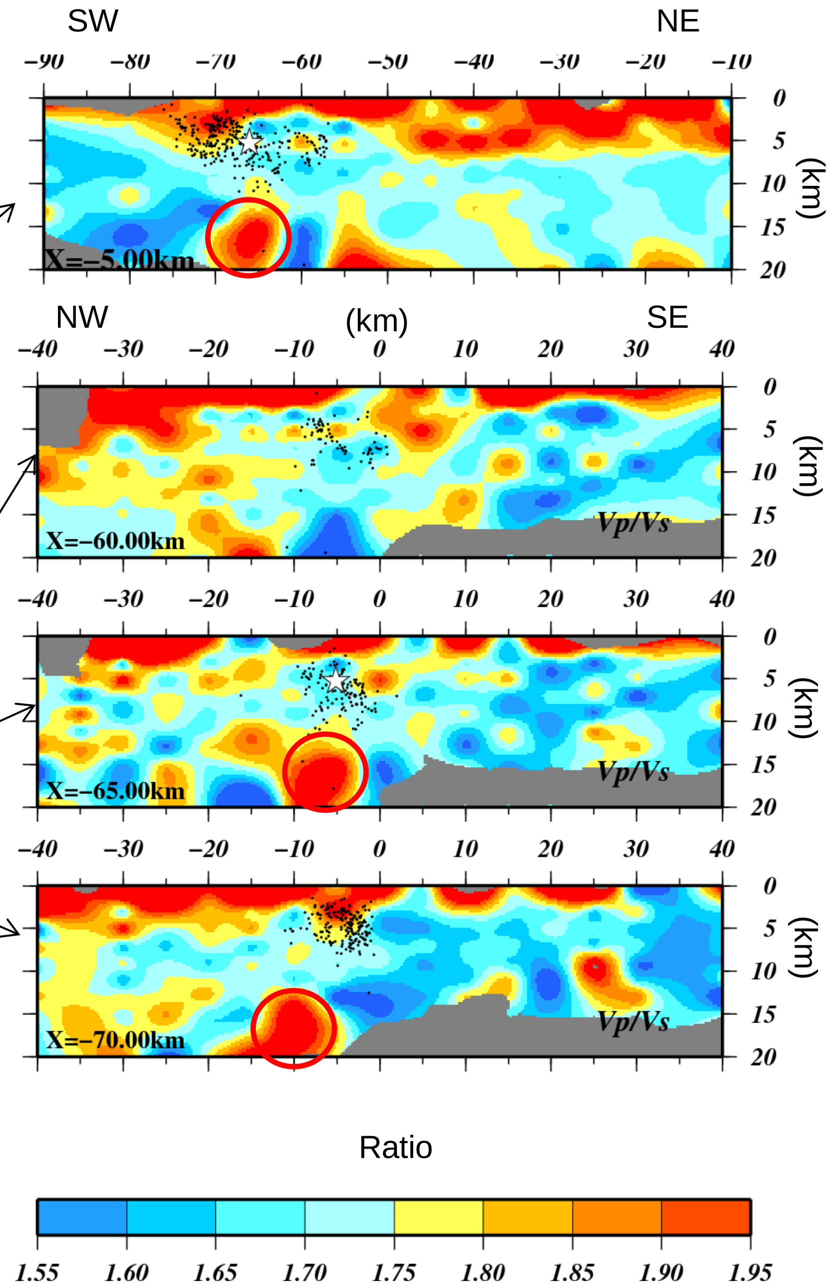

Enescu and Takeda, 2012

Far field triggering
(the static stress influence becomes small/very small
Yukutake et al., 2011; Miyazawa, 2011; Enescu, Obara
et al., in prep.)

Dynamic triggering in south Kyushu by the 2011 Tohoku earthquake (about 1350 km from the Tohoku earthquake hypocenter)

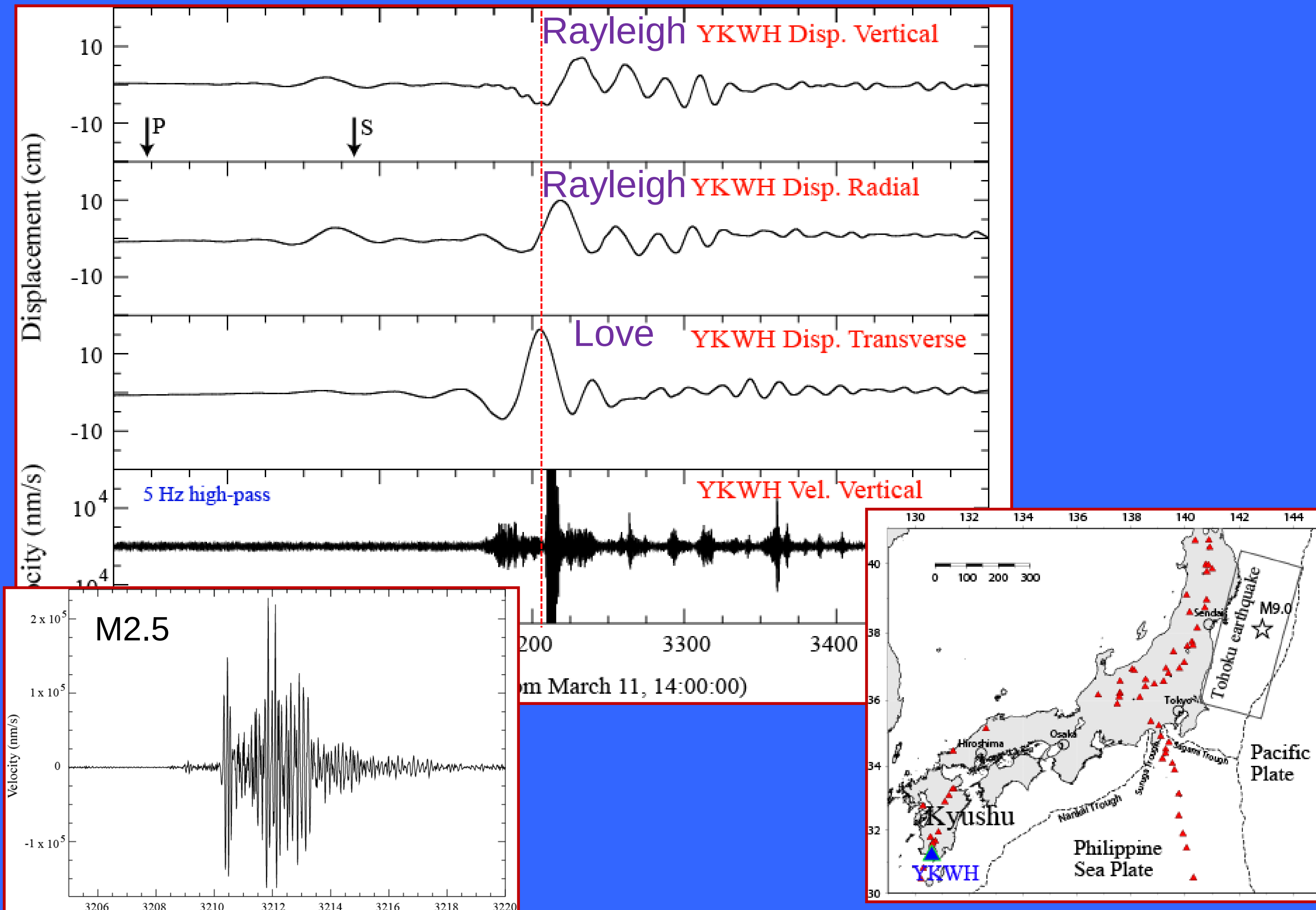

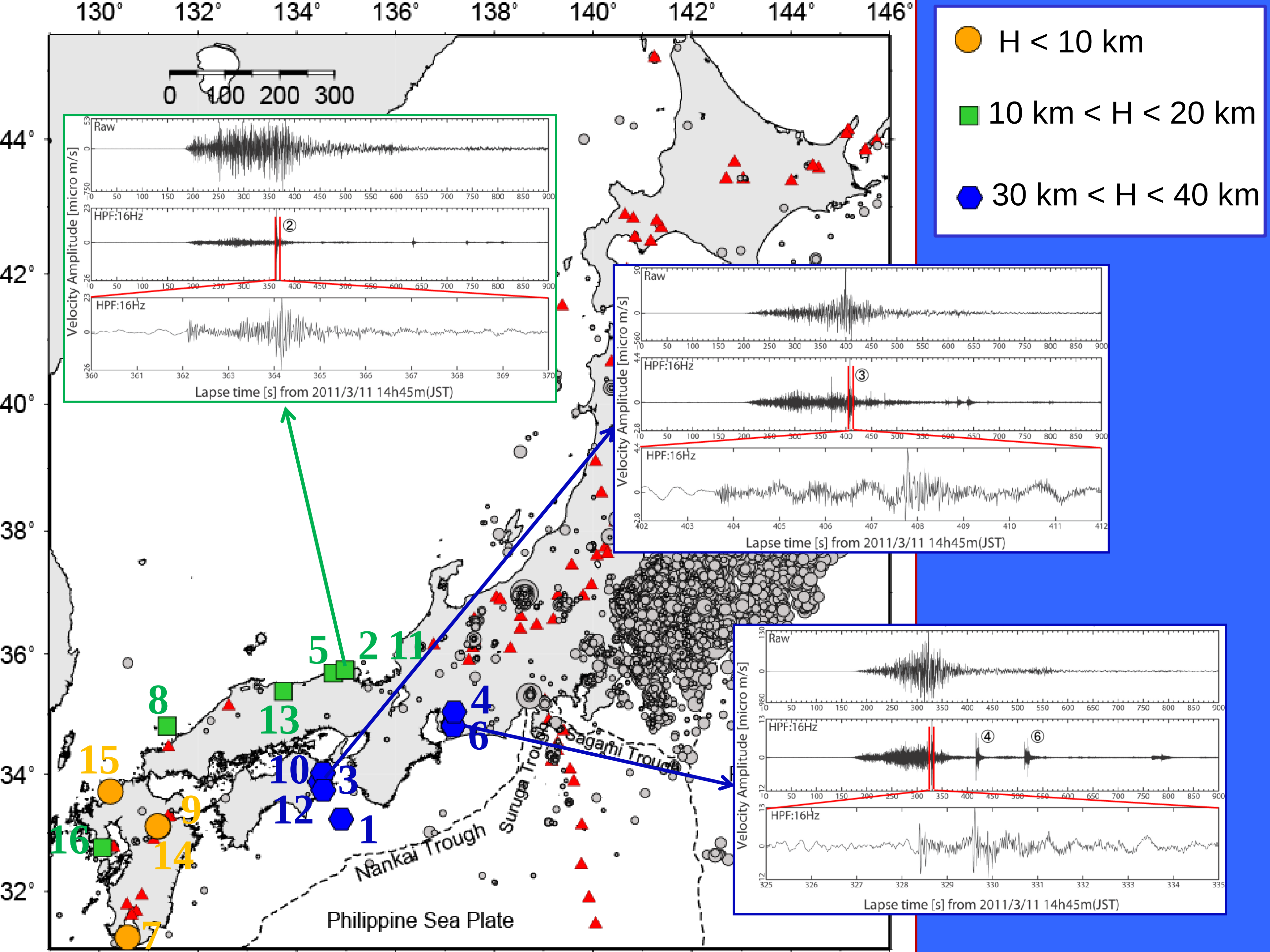

H < 10 km
10 km < H < 20 km
30 km < H < 40 km
Philippine Sea Plate
Nankai Trough
Suruga Trough
Sagami Trough
Raw
HPF:16Hz
Velocity Amplitude [micro m/s]
Lapse time [s] from 2011/3/11 14h45m(JST)

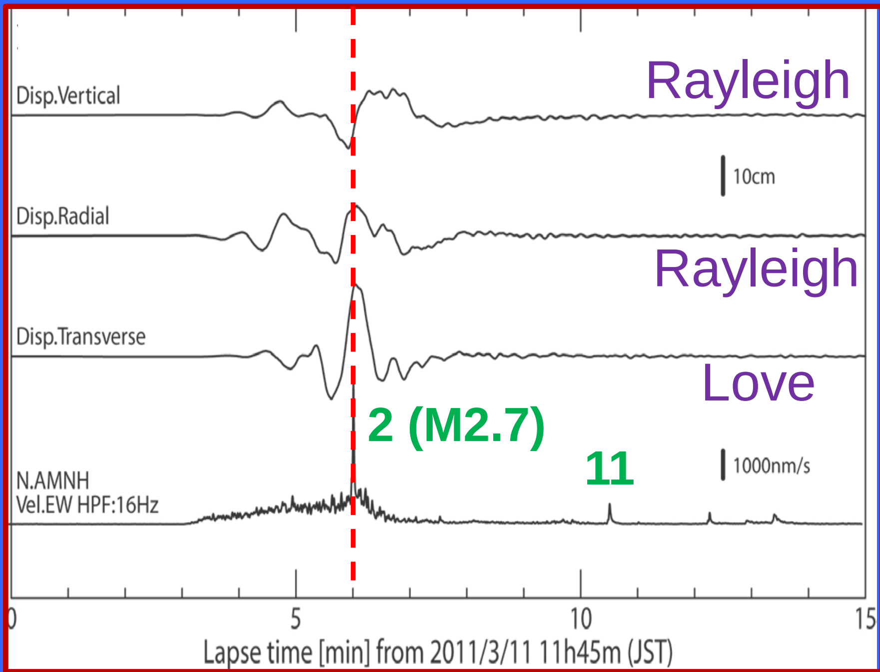

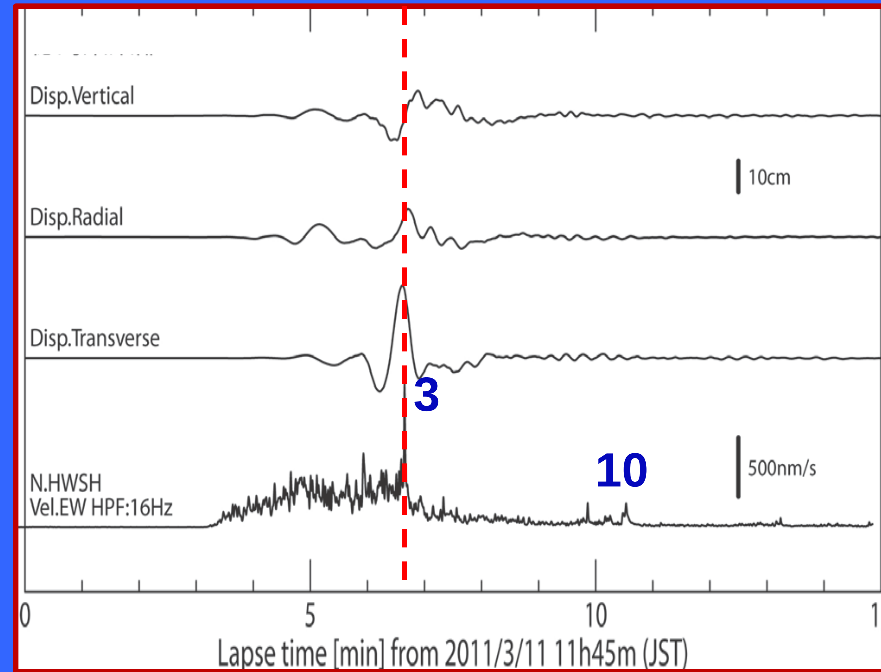

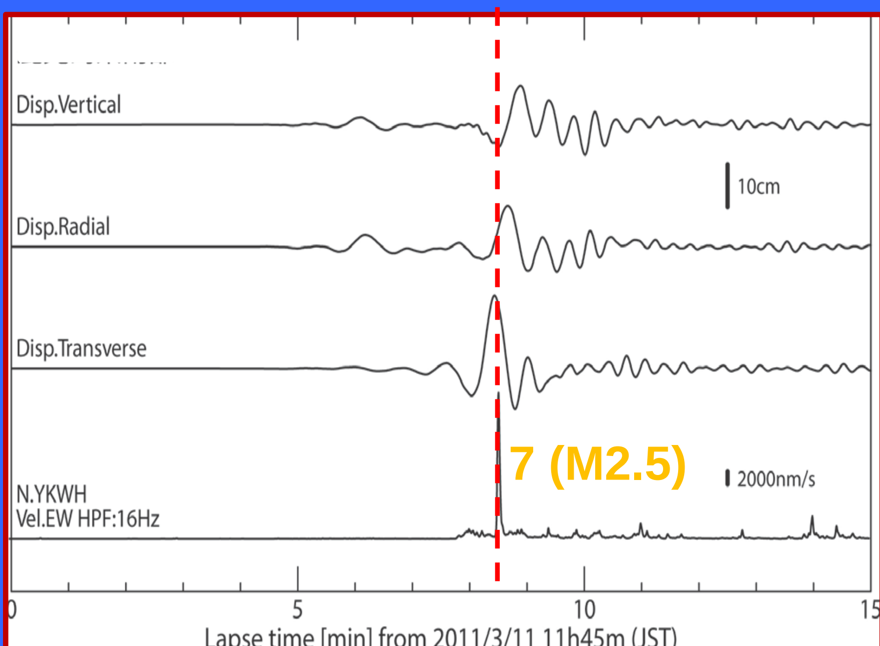

Remote earthquake activation during the passage of seismic waves from Tohoku earthquake.

There is a good correspondence with the transverse component displacement (Love waves).

Checking remote triggering using the JMA catalog

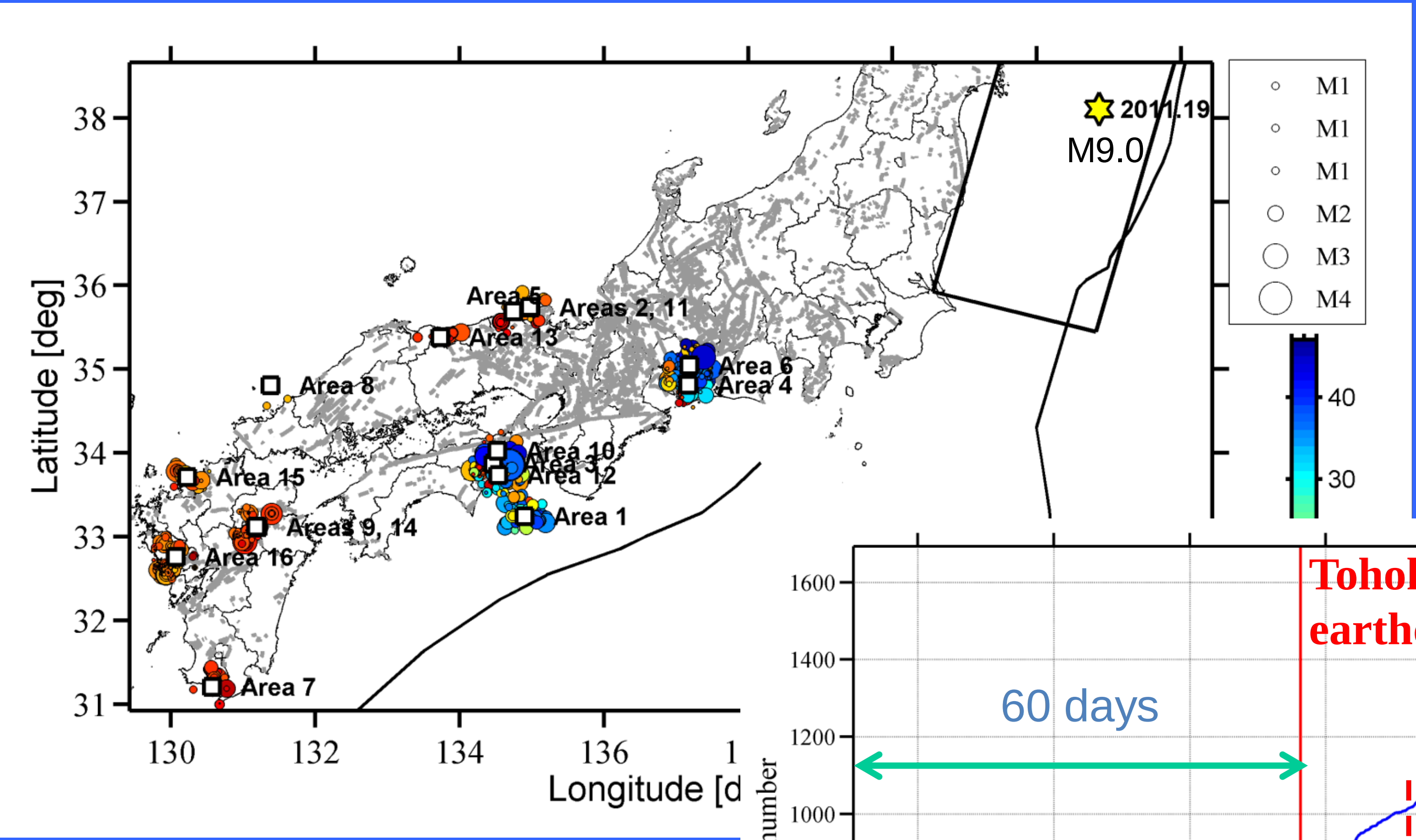

30 km radius selection around each triggered event (white square)

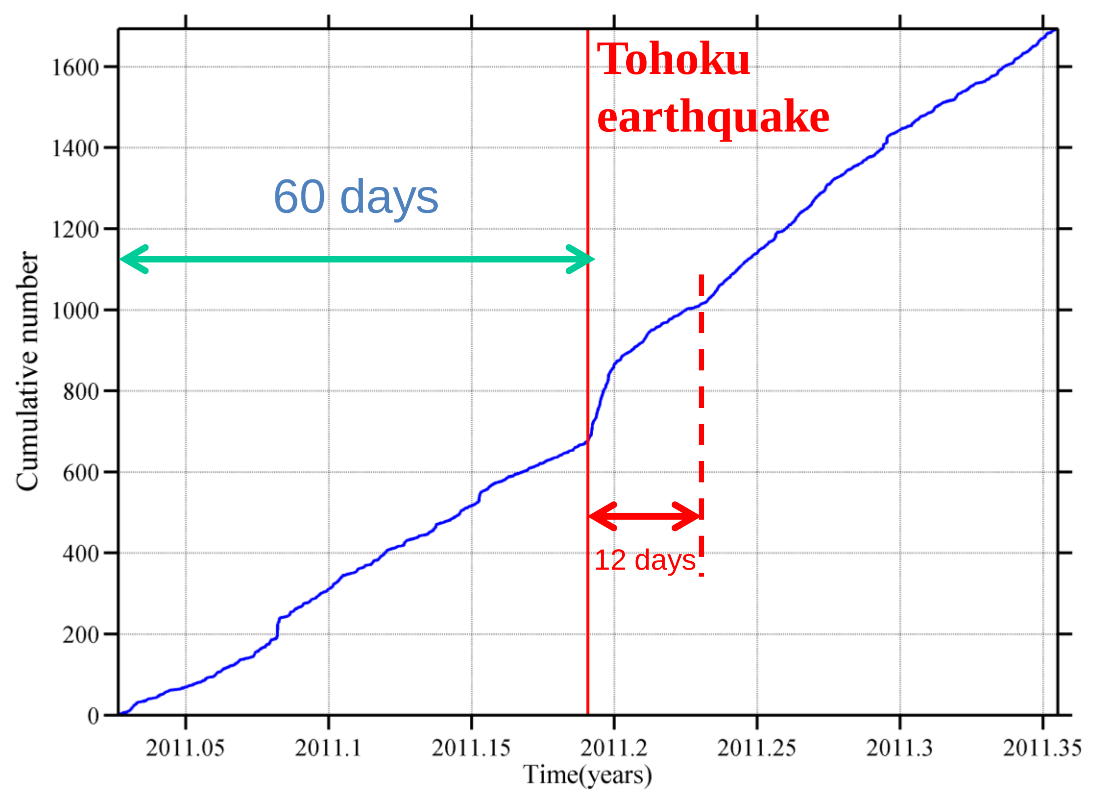

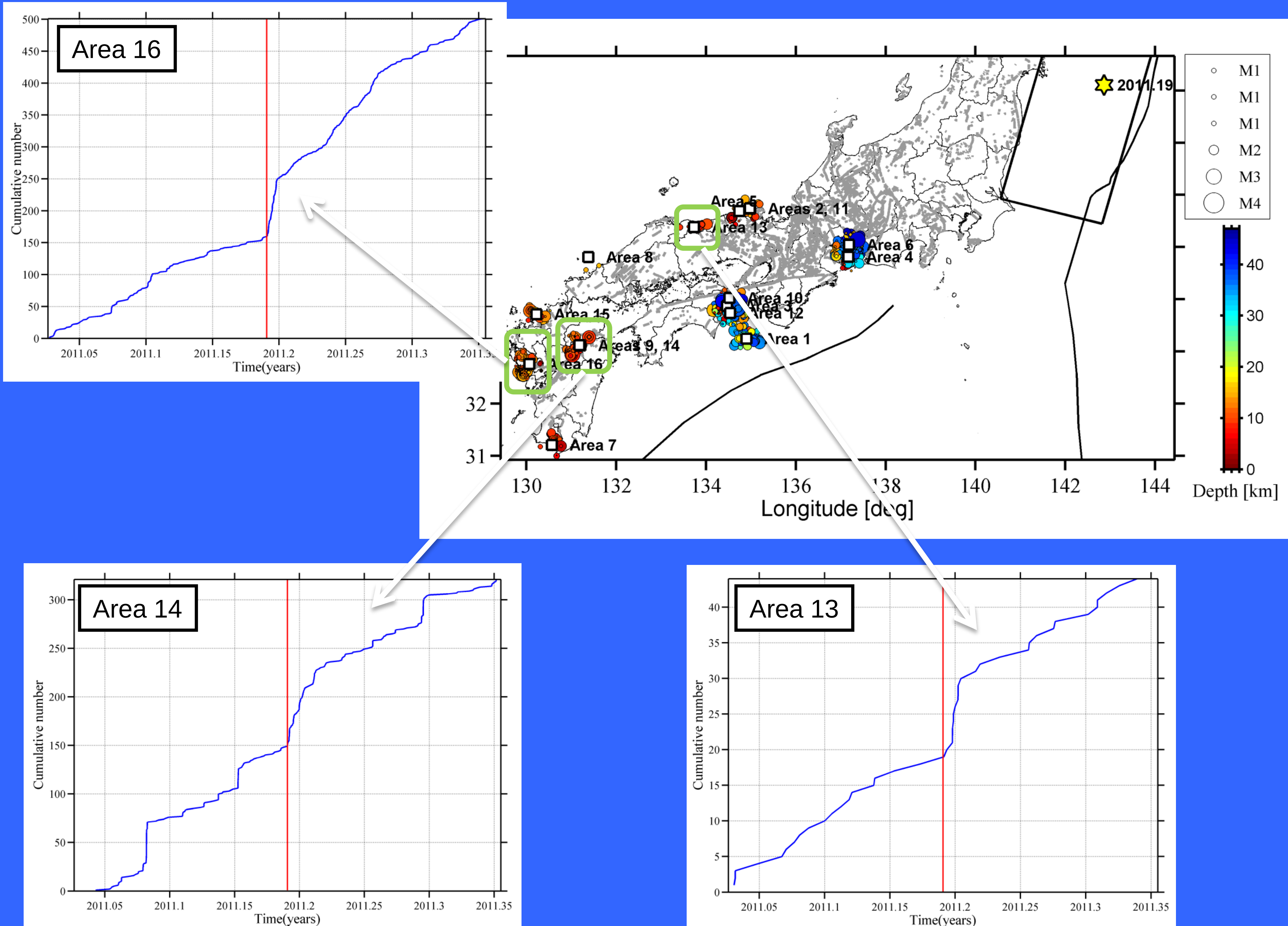
Area 16
Cumulative number
Time(years)
2011.19
M1
M1
M1
M2
M3
M4
Depth [km]
Longitude [deg]
Area 5
Areas 2, 11
Area 13
Area 6
Area 4
Area 8
Area 10
Area 3
Area 12
Area 15
Area 1
Areas 9, 14
Area 16
Area 7
Area 14
Area 13

Dynamic stresses during the passage of surface waves from mainshock (southern Kyushu, ~ 1350 km from Tohoku epicenter)

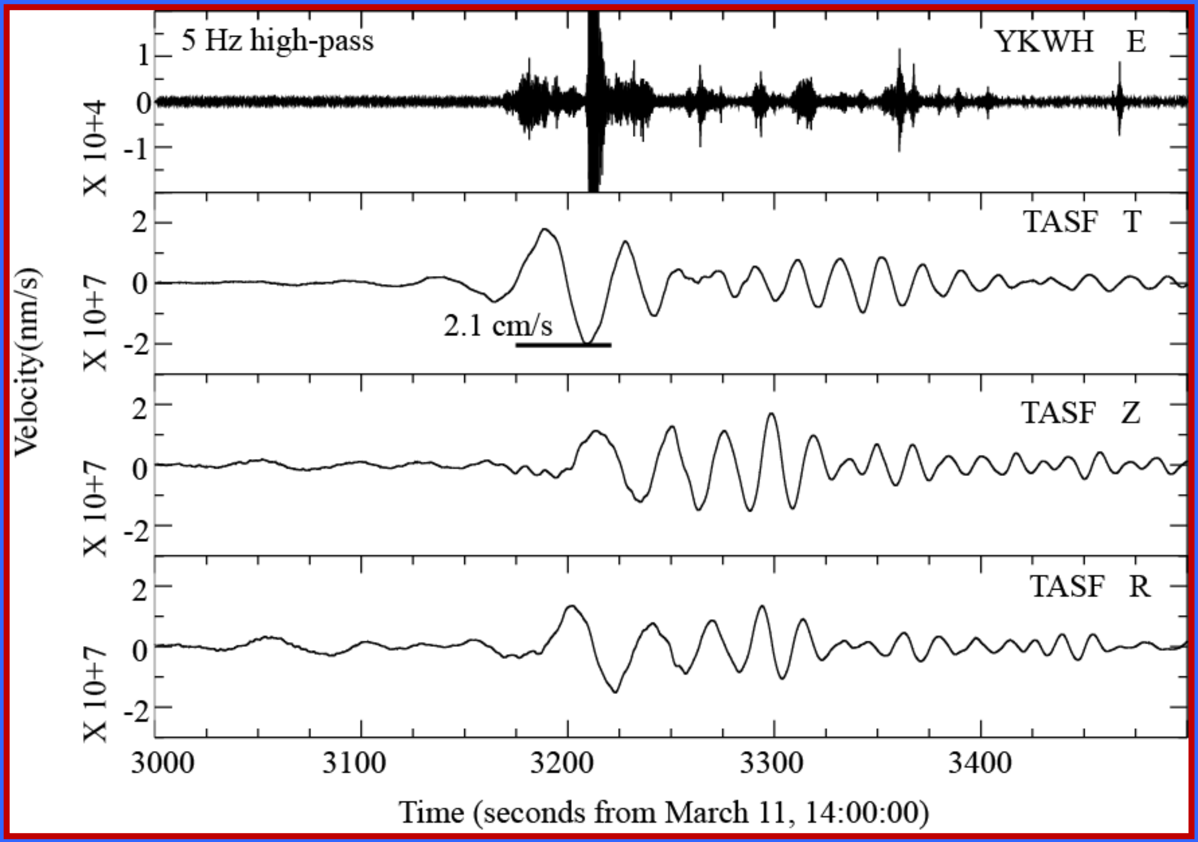

$$\sigma_d = \frac{G\dot{u}}{v_s}$$

G – shear modulus (30 GPa)

Vs – phase velocity $\left(4.1\ ^{km}/_{s}\right)$

$\dot{u}$ – peak particle velocity $(2.1\ ^{cm}/_{s})$

σ_d = 154 kPa (0.15 MPa)

The Coulomb static stress changes are on the order of 0.002 MPa (about 100 times less than the dynamic ones).

A few slides explaining more detailed dynamic stress calculations that we did for tremor and we plan for triggered earthquakes as well…

Systematic study of teleseismic triggered tremor in SW Japan

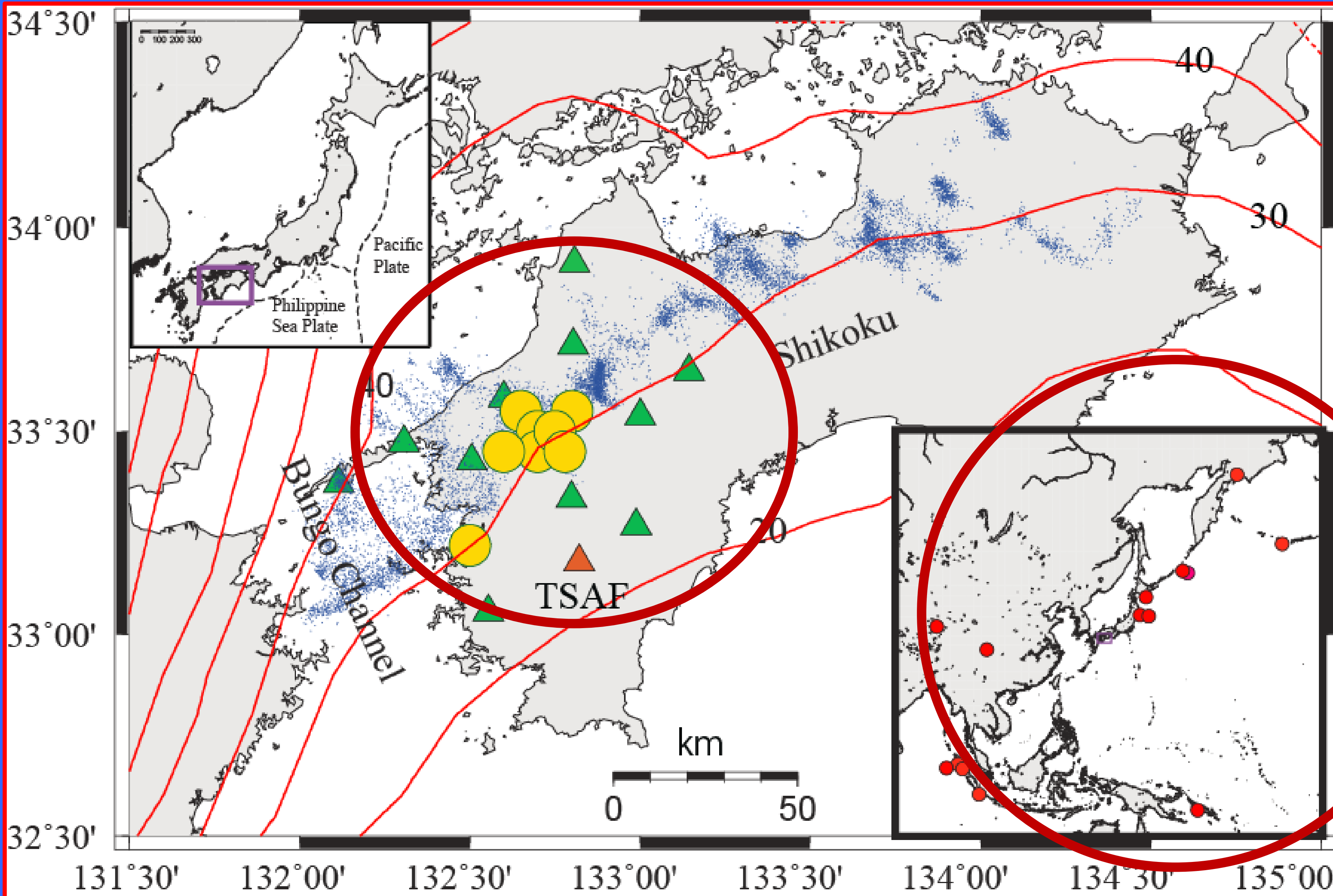

18 teleseismic events show associated triggered tremor

Enescu et al., in prep.

Setting of the problem in the Nankai region

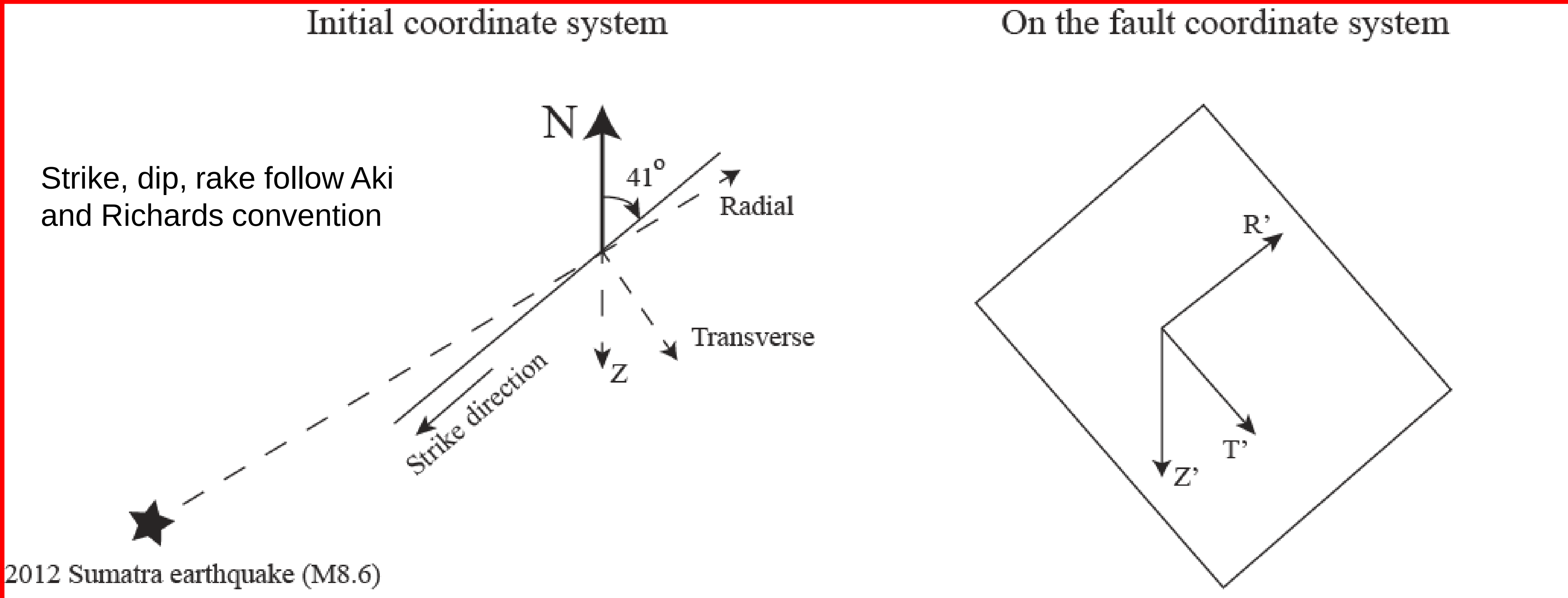

Strike, dip, rake follow Aki and Richards convention

The coordinates are transformed by a rotation around Z-axis, followed by a rotation around the T'-axis.

The strains and stresses calculated in the (Radial, Transvers, Vertical) coordinate system are rotated in to the on-fault coordinate system, as shown in the figure.

Dynamic stress calculation

Model (Rayleigh wave)

Model (Love waves)

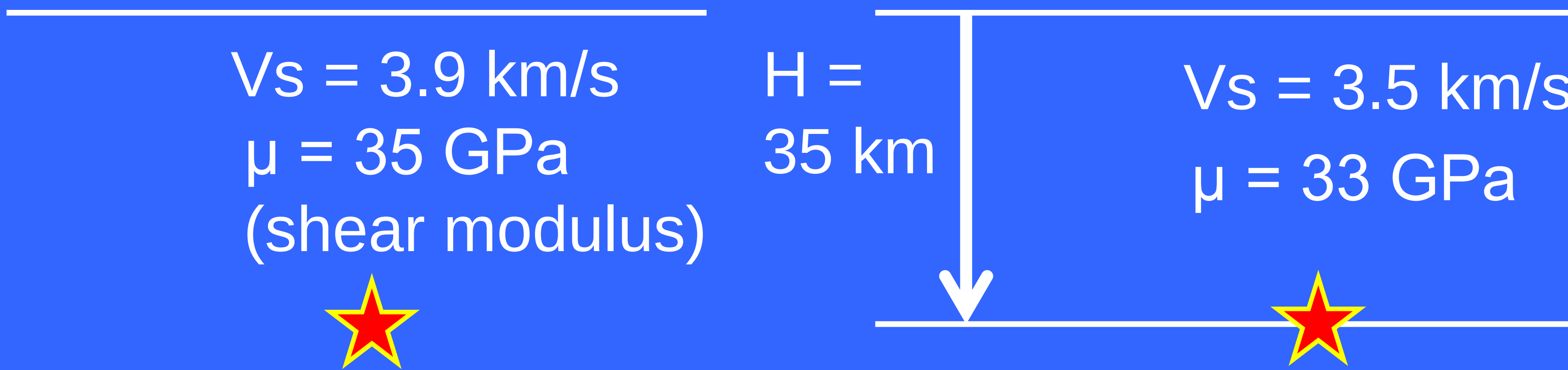

Poisson solid

Vs = 4.5 km/s

μ = 69 GPa

Coefficient of friction = 0.2 for dynamic $\triangle CFS$

We calculate dynamic stress changes at depth, due to low-frequency displacements (V, R, T) at the surface. We assume simple velocity models to calculate the strain and stress at depth. Method similar with that used by Hill, 2012; Miyazawa & Brodsky, 2008; Gonzalez-Huizar & Velasco, 2011.

Modeling of dynamic stress (2012 Sumatra earthquake, M8.6)

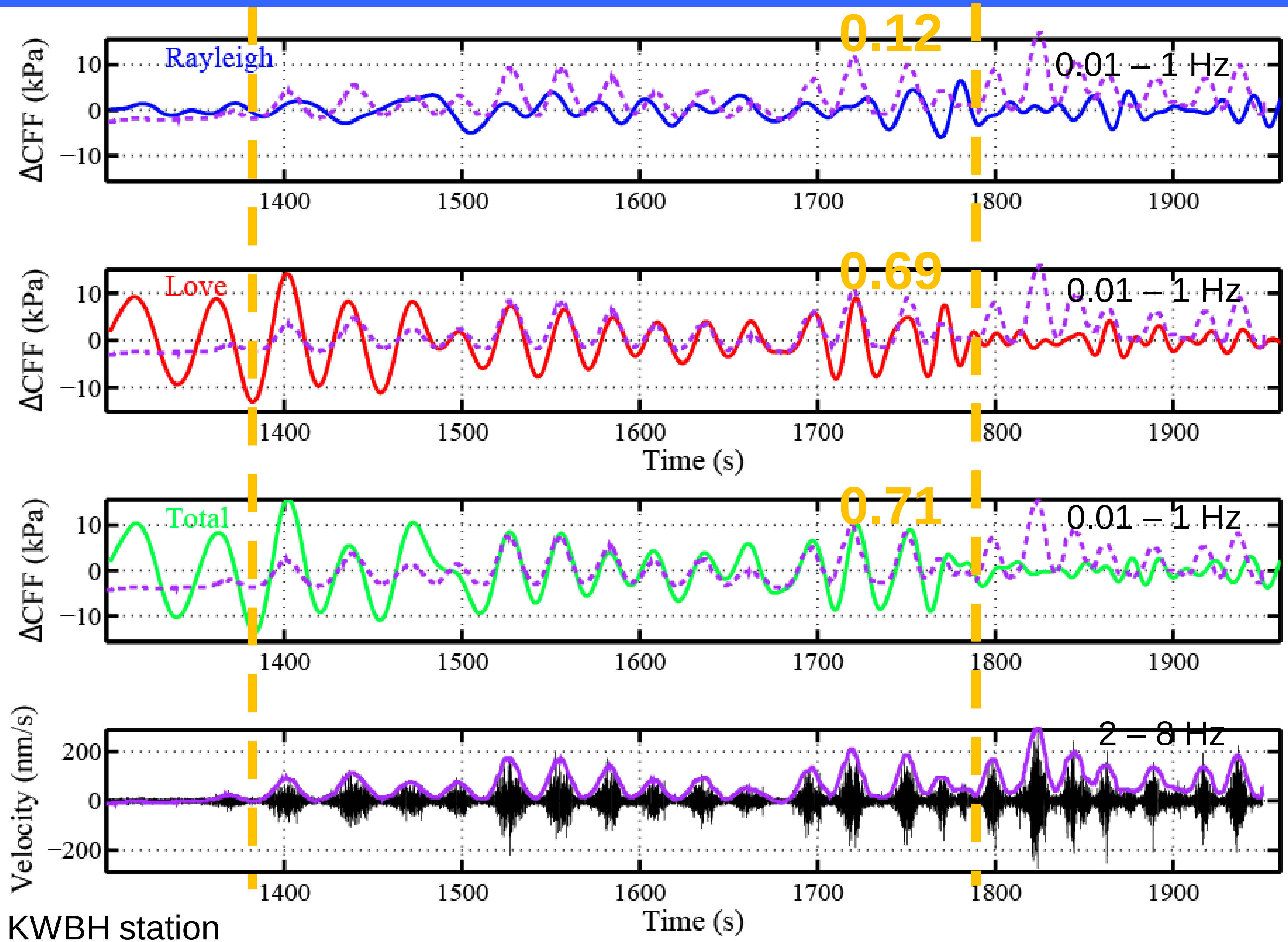

KWBH station

Conclusions

Temporal decay:

- power-law Omori-law from the earliest times (minutes);
- extremely small c-values that can be explained by slip heterogeneity;
- imaging in both time domain and energy domain.

Spatial features:

- migrations – as indication of aseismic processes (e.g., afterslip following the Tohoku-oki megaquake);
- Static stress triggering in the near field can explain well the overall seismicity after Tohoku-oki EQ, at larger distances the dynamic effects become stronger;
- fluids facilitate triggering in some areas in NE Japan.